

Wall-modeled LES of Turbulent Flows Past Airfoils and Periodic Hills

Wei Gao¹, Wan Cheng^{1,2}

Ravi Samtaney¹

(Email: Ravi.Samtaney@kaust.edu.sa)

¹ Mechanical Engineering, PSE Division

King Abdullah University of Science & Technology

² Graduate Aerospace Laboratories

California Institute of Technology

August 11, 2020

AMS Seminar, NASA Ames Research Center

Collaborators: Prof. D. I. Pullin, Caltech

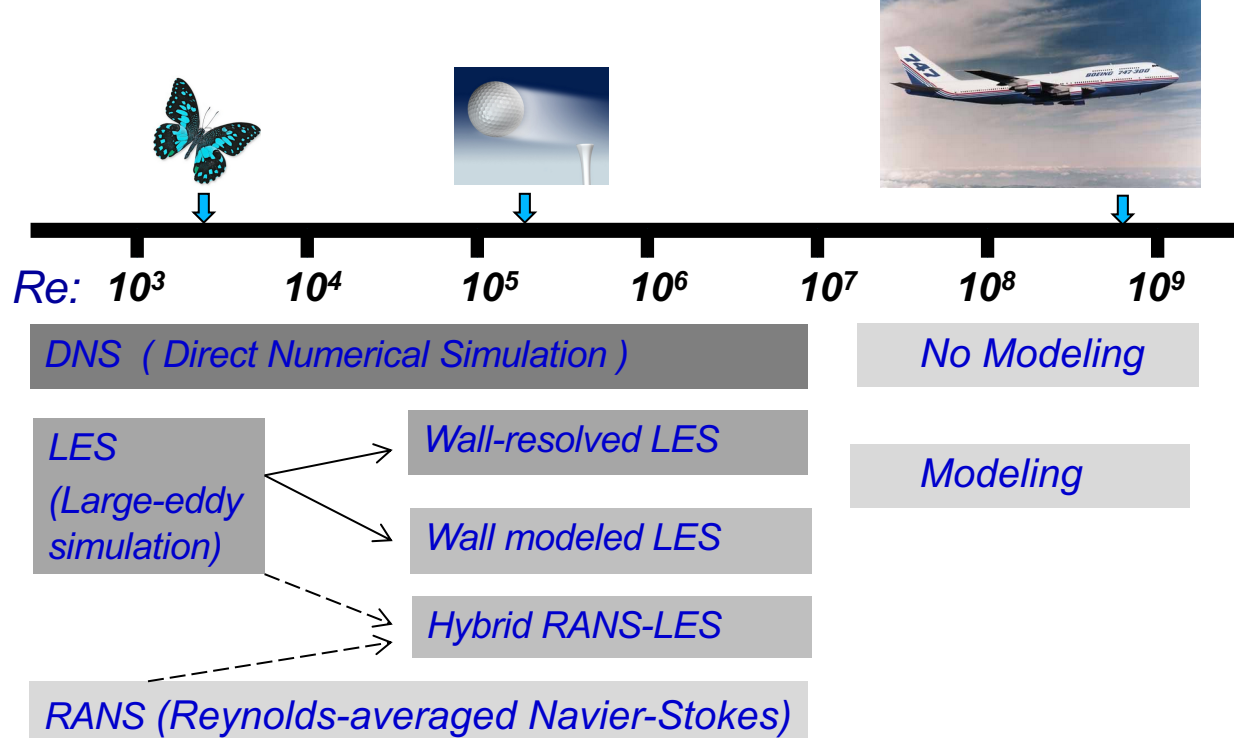
Prof. Wei Zhang, Zhejiang Sci-Tech University

Outline

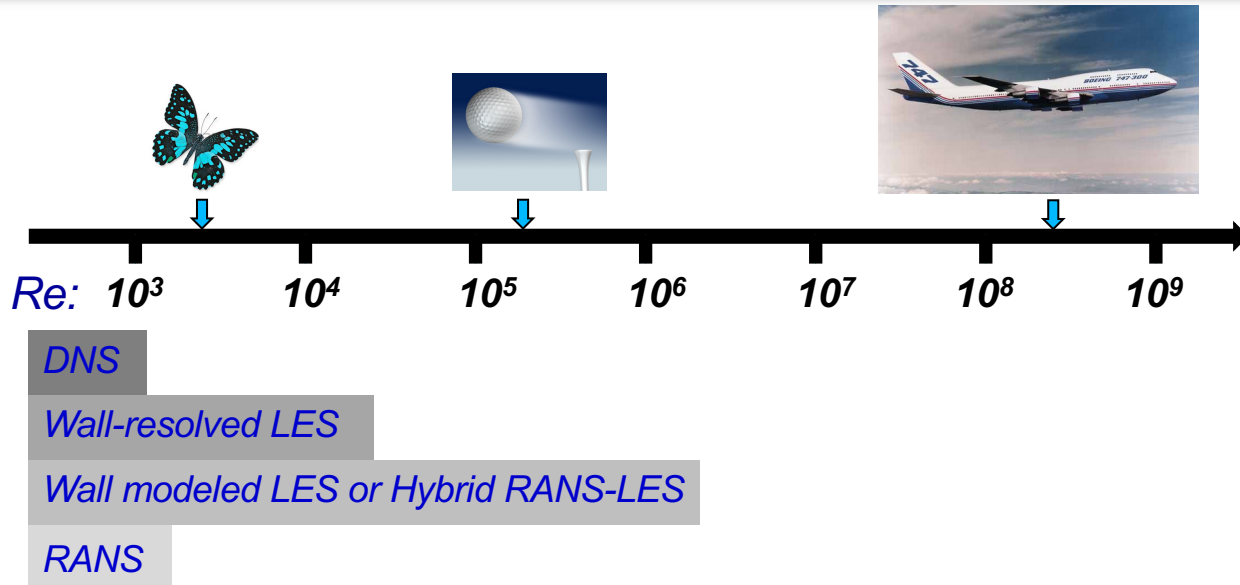
- Introduction
- SGS and Wall Models
 - *Virtual wall boundary conditions*
- WMLES of flow past airfoils
- WMLES of flow past periodic hills

Conclusion

Fluid Mechanics: Reynolds number (Re)

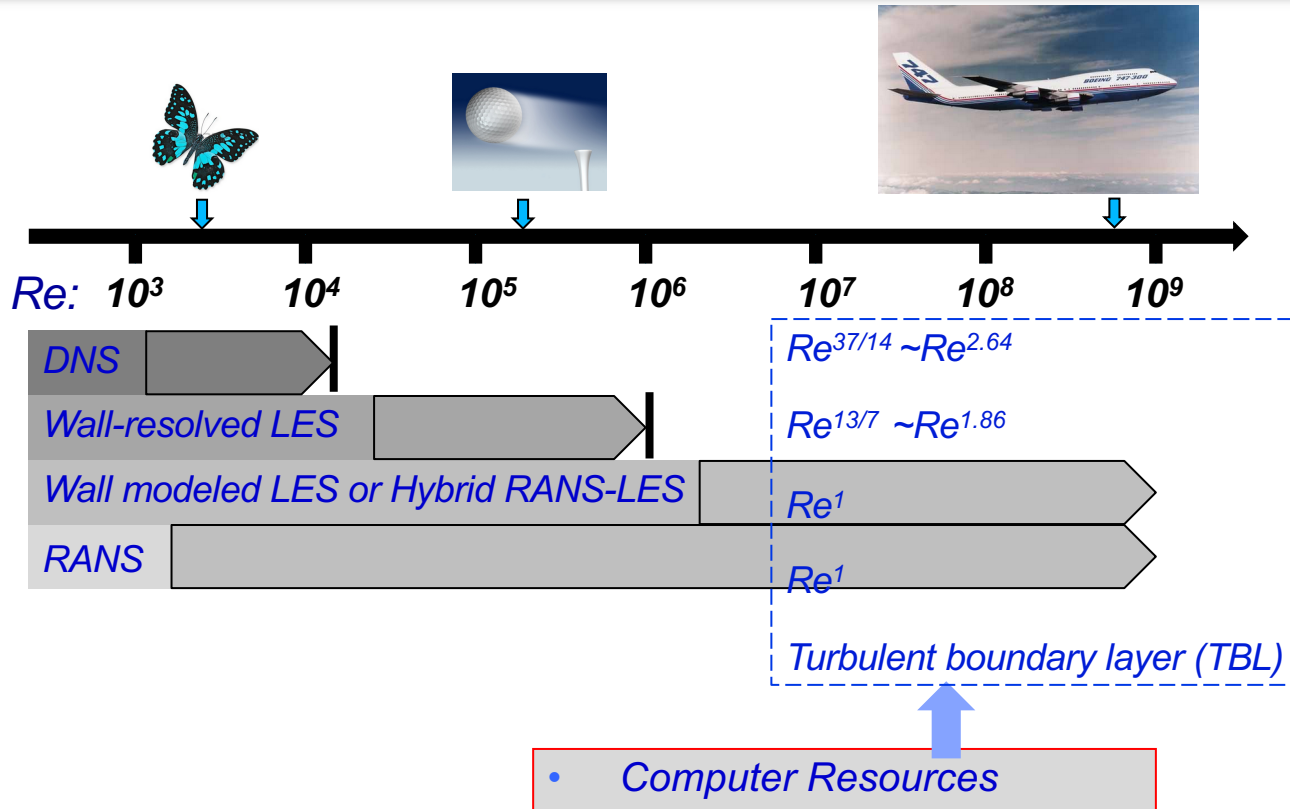


Fluid Mechanics: Reynolds number (Re)

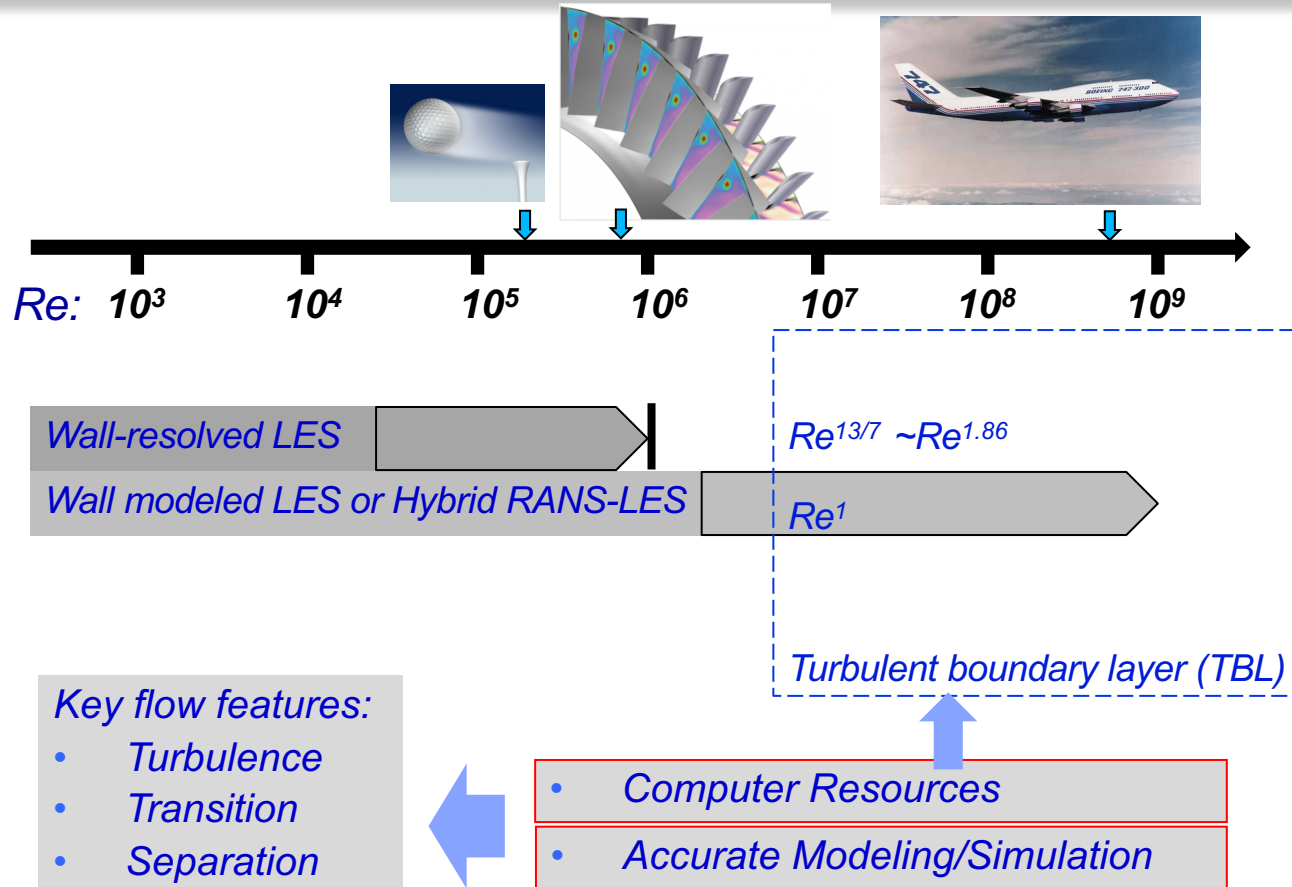


- Computer Resources

Fluid Mechanics: Reynolds number (Re)

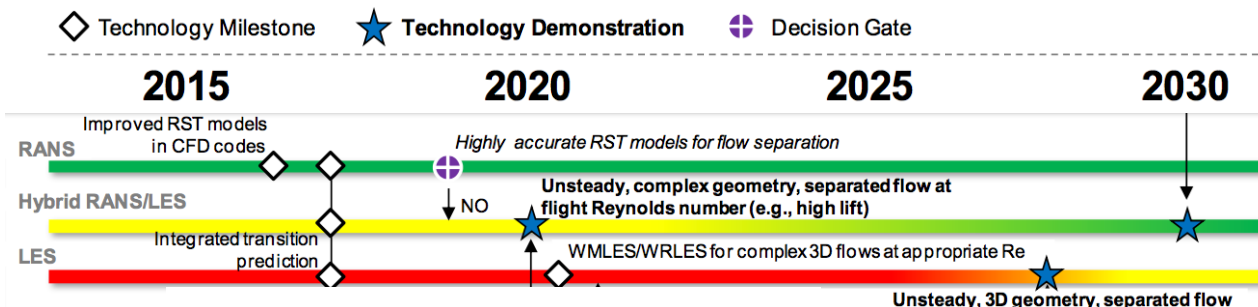
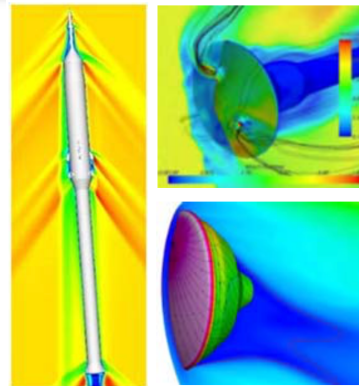


Fluid Mechanics: Reynolds number (Re)

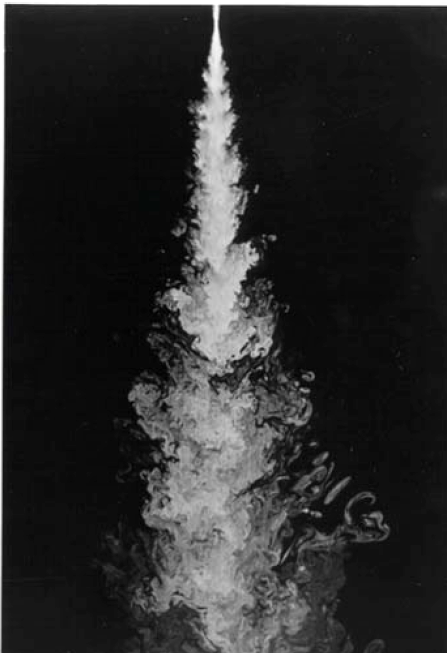


NASA: Critical challenges in CFD ---- Separation

- NASA's 2014 Aerosciences: Top three challenges
 - Prediction of unsteady separated flows
 - Aero-plume interaction prediction
 - Aerothermal prediction
- NASA CFD 2030 VISION

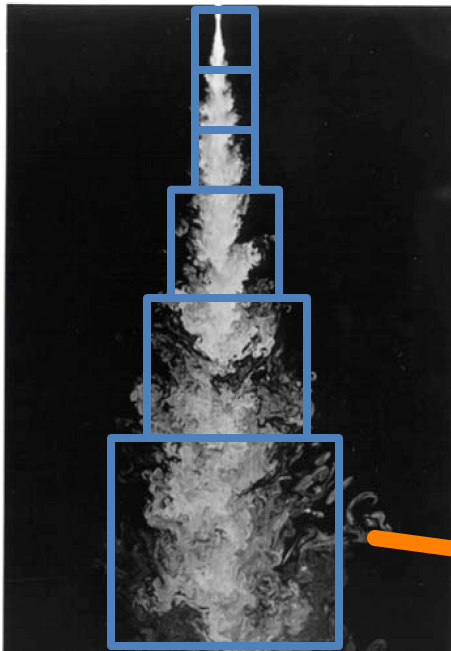


Direct Numerical Simulation (DNS) vs Large-Eddy Simulation (LES)

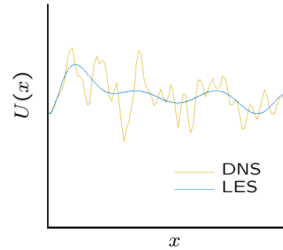


*Re = 10k (Dimotakis et al.
1983)*

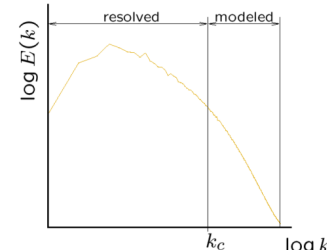
Direct Numerical Simulation (DNS) vs Large-Eddy Simulation (LES)



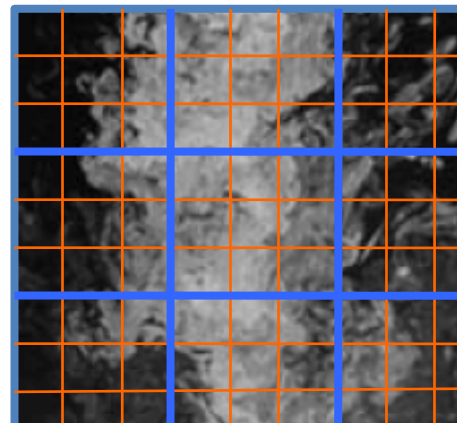
$Re = 10k$ (Dimotakis et al.
1983)



physical space: fine-scale fluctuations not resolved, their influence is modeled.



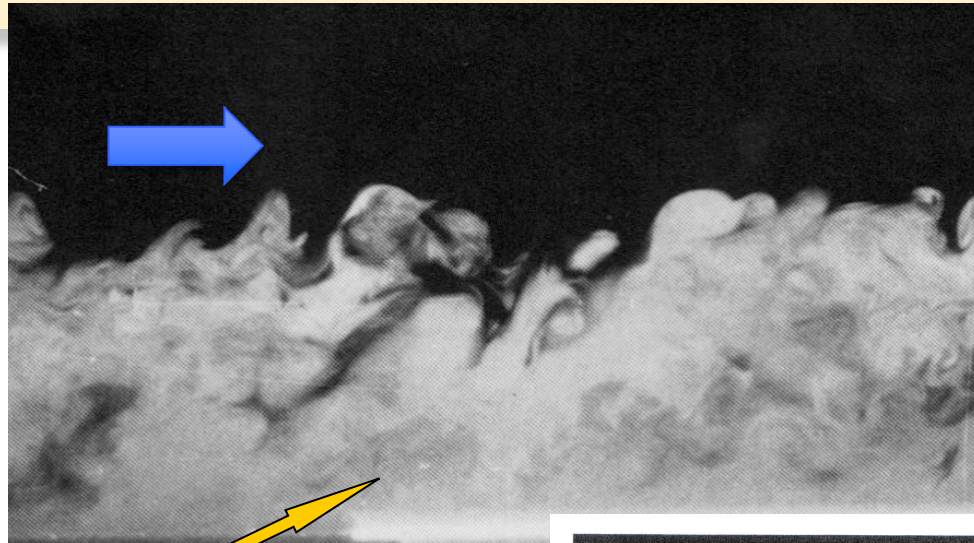
spectral space: resolved range, $k < k_c$ (cutoff wavenumber k_c), subgrid range $k > k_c$.



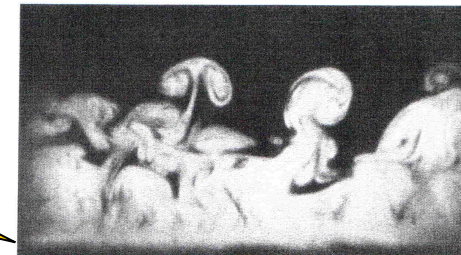
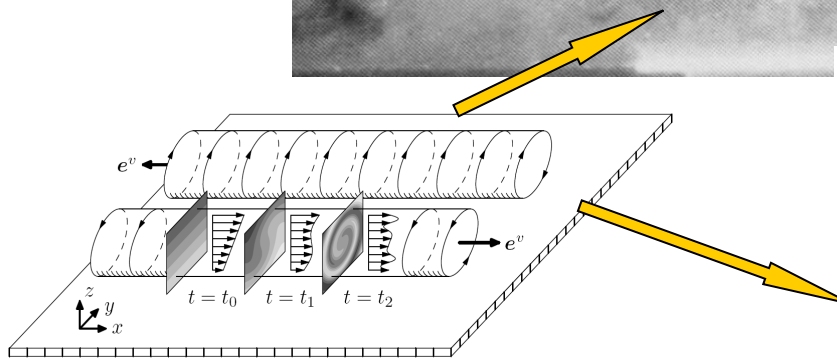
DNS

LES

LES for wall-bounded flows

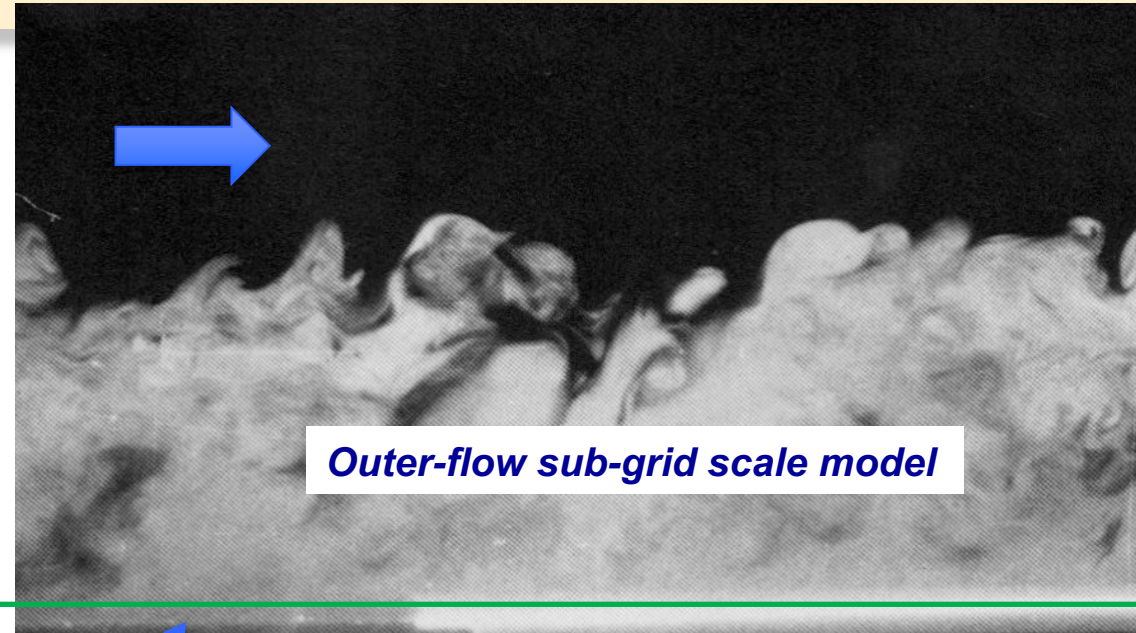


(Falco 1977)



Head & Bandyopadhyay (1981)

LES for wall-bounded flows



**Wall-modeled
region**

True wall

(Falco 1977)

Filtered Navier-Stokes Equations

- Apply filtering operation to incompressible Navier-Stokes equations

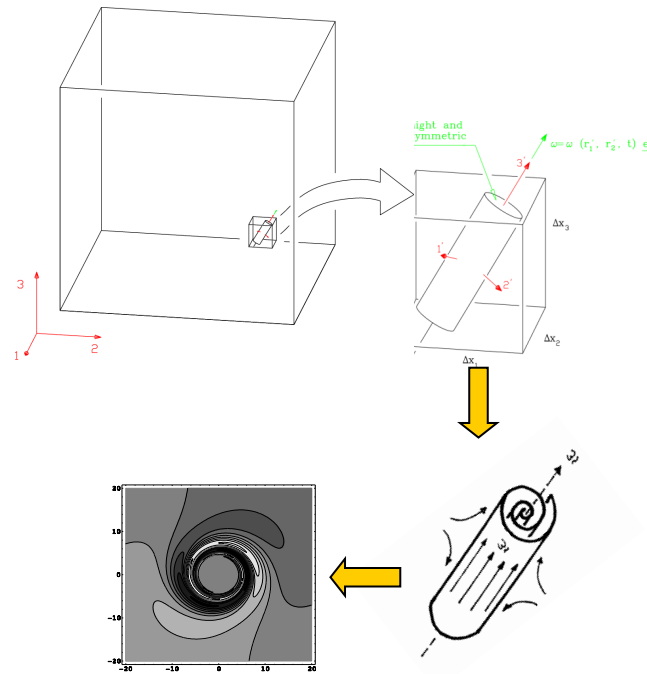
$$\begin{aligned}\frac{\partial \tilde{u}_i}{\partial x_i} &= 0 \\ \frac{\partial \tilde{u}_i}{\partial t} + \frac{\partial}{\partial x_j} (\tilde{u}_i \tilde{u}_j) &= -\frac{\partial \tilde{p}}{\partial x_i} + \nu \frac{\partial^2 \tilde{u}_i}{\partial x_i^2} \\ \frac{\partial \tilde{u}_i}{\partial t} + \frac{\partial}{\partial x_j} (\tilde{u}_i \tilde{u}_j) &= -\frac{\partial \tilde{p}}{\partial x_i} - \frac{\partial}{\partial x_i} \underbrace{(\tilde{u}_i \tilde{u}_j - \tilde{u}_i \tilde{u}_j)}_{T_{ij}} + \nu \frac{\partial^2 \tilde{u}_i}{\partial x_i^2} \\ \tilde{u}_i \tilde{u}_j(x, t) &\equiv \int_{-\infty}^{\infty} \mathcal{G}(x' - x) u_i(x') u_j(x') dx' \neq \tilde{u}_i \tilde{u}_j\end{aligned}$$

- T_{ij} ``unresolved stresses'' must be modeled: this is the ``closure problem''
- Filtering process on NS equations is strictly formal: no particular filter is actually needed

Explicit SGS model: stretched-vortex model

- Structure-based approach
- Subgrid motion represented by nearly axisymmetric vortex tube within each cell
- Local solution of NS equations for stretched-spiral vortex
 - Lundgren (1982), Pullin & Lundgren (2001)
- Subgrid stress:

$$\tau_{ij} = (\delta_{ij} - e_i^\nu e_j^\nu) K,$$



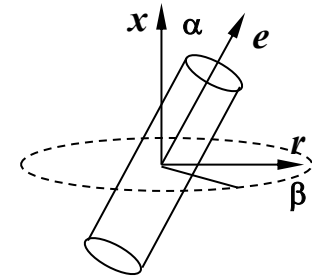
$$K = \int_{k_c}^{\infty} E(k) dk = \frac{1}{2} \mathcal{K}'_0 \Gamma [-1/3, \kappa_c^2], \mathcal{K}'_0 = \mathcal{K}_0 \epsilon^{2/3} \lambda_v^{2/3}$$

Model parameters

- Subgrid energy spectrum (Lundgren, 1982)

$$E(k) = \mathcal{K}_0 \epsilon^{2/3} k^{-5/3} \exp[-2k^2\nu/(3|\tilde{a}|)]$$

$$\tilde{a} = \tilde{S}_{ij} e_i^v e_j^v, \quad \tilde{S}_{ij} = \frac{1}{2} \left(\frac{\partial \tilde{u}_i}{\partial x_j} + \frac{\partial \tilde{u}_j}{\partial x_i} \right)$$



- Parameters obtained from resolved-scale, second order velocity structure-functions (Lesieur et al)

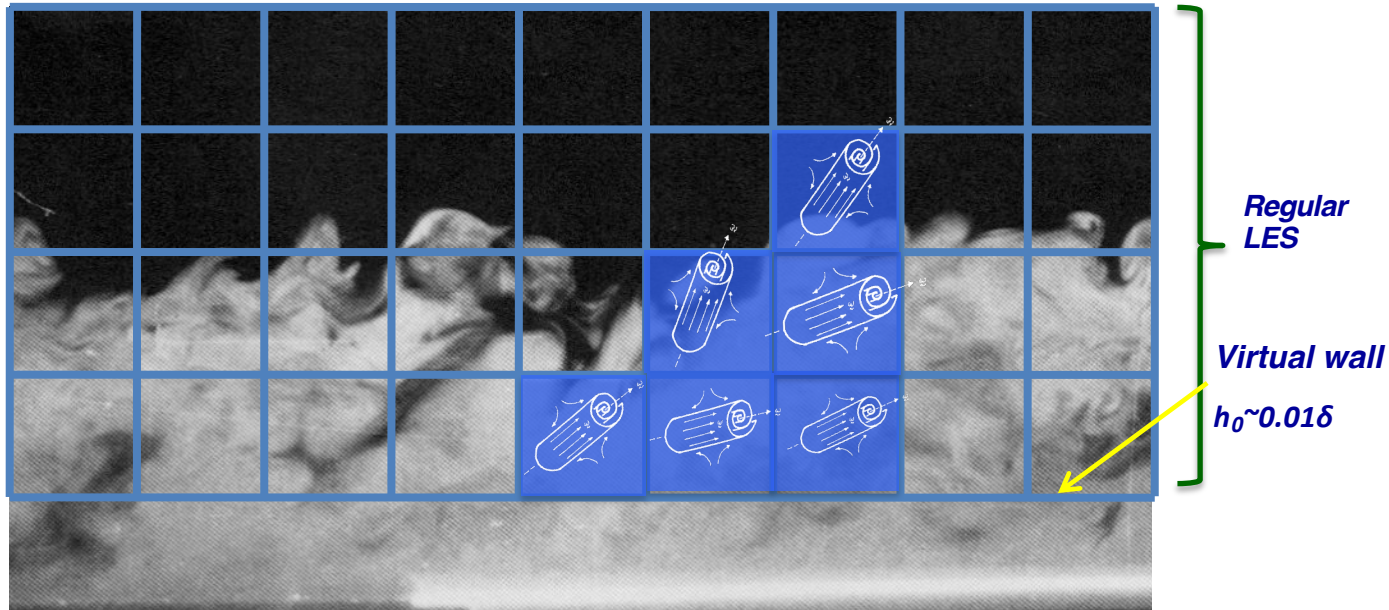
$$\mathcal{K}_0 \epsilon^{2/3} = \frac{\overline{\mathcal{F}_2}(\Delta)}{\Delta^{2/3} A}, \quad A = 4 \int_0^\pi s^{-5/3} (1 - s^{-1} \sin s) ds \approx 1.90695$$

$$\overline{\mathcal{F}_2}(\Delta) = \frac{1}{6} \sum_{j=1}^3 \left(\delta \tilde{u}_1^+{}^2 + \delta \tilde{u}_2^+{}^2 + \delta \tilde{u}_3^+{}^2 + \delta \tilde{u}_1^-{}^2 + \delta \tilde{u}_2^-{}^2 + \delta \tilde{u}_3^-{}^2 \right)_j,$$

- Align SGS vortex axis with principal extensional eigenvector of \tilde{S}_{ij}
- See Misra & Pullin (1997), Voelkl & Pullin (2000) for details

LES + wall model for high Re flow

Outer flow: LES with stretched-vortex SGS model



LES + wall model for high Re flow

Wall-model based on idea of attached eddies (Townsend)

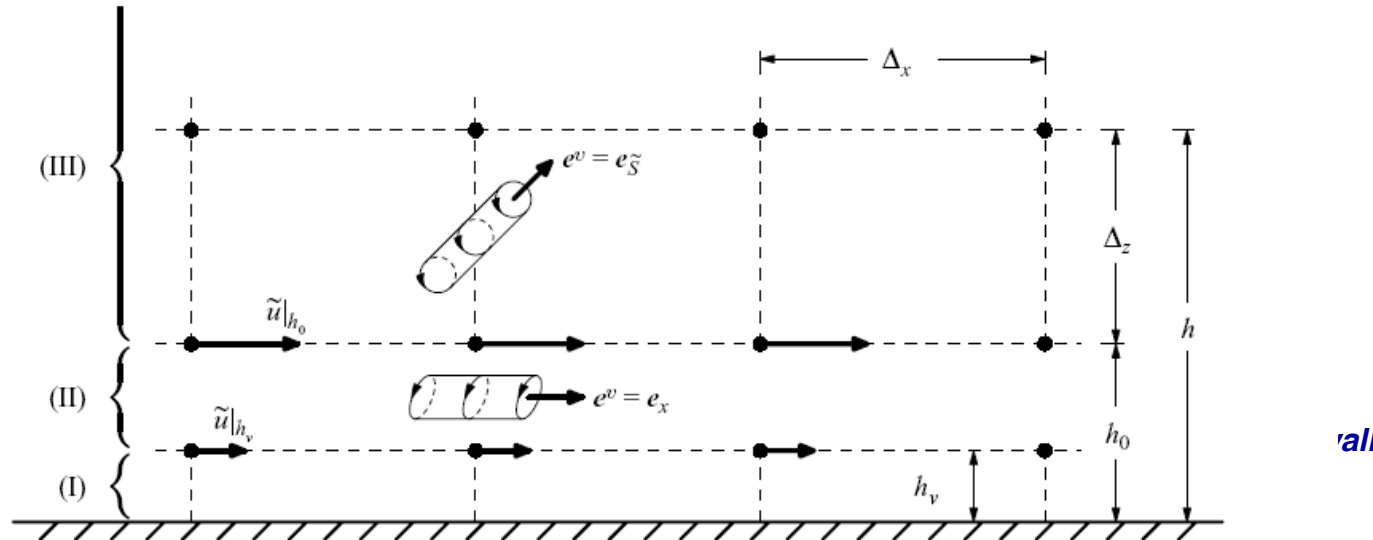


FIGURE 1. Schematic showing the near-wall set-up: h_0 locates the lifted virtual wall, where boundary conditions are applied; h locates the input plane to the wall shear stress equation, (3.10); h_v locates the outer edge of the viscous sublayer; e^v is the alignment of SGS vortices in their respective regions.

wall

el

Wall Model

Wall Model – Essential Idea



- Inner scaling combined with wall normal integration filter

$$\frac{\tilde{q}}{u_\tau} = F(z^+), \quad z^+ \equiv \frac{z}{l^+} = \frac{zu_\tau}{\nu}. \quad \Longrightarrow \quad \frac{\partial \langle q \rangle}{\partial t} = \frac{\tilde{q}|_h}{2\eta_0} \frac{\partial \eta_0}{\partial t}.$$

- Main points to note
 - Mean flow aligned with streamwise direction
 - Classical inner scaling
 - Near wall integration approach

Wall Model

- ODE for wall shear stress (or u_τ) at every wall point $u_\tau^2 \equiv \nu \eta_0$ $\eta_0 \equiv \left. \frac{\partial \tilde{u}}{\partial z} \right|_0$
 - Wall-normal integration of streamwise momentum equation
 - Top-hat filter normal to the wall, $0 < z < h$: $h = \Delta z > h_0$
 - Local inner-scaling reduction for unsteady term

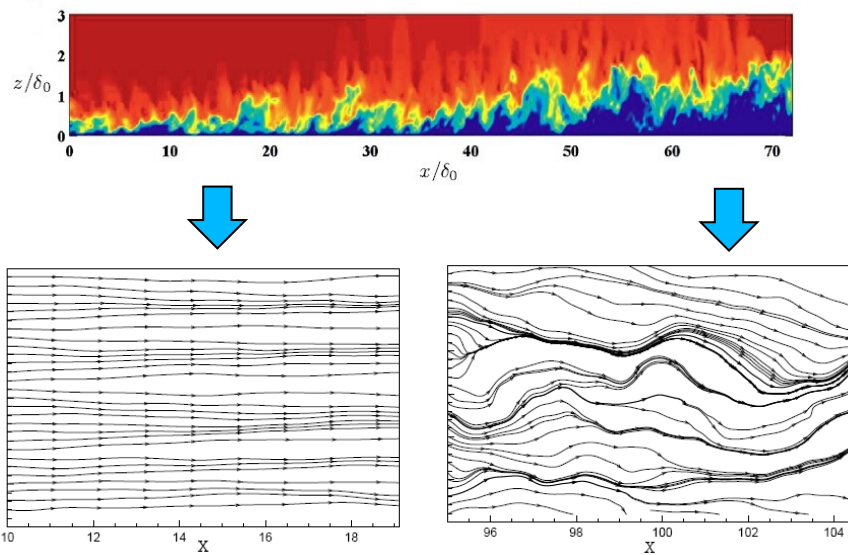
$$\frac{\partial \eta_0}{\partial t} = \frac{2\eta_0}{\tilde{u}|_h} \left[-\frac{\partial \tilde{u}\tilde{u}|_h}{\partial x} - \frac{\partial \tilde{u}\tilde{v}|_h}{\partial y} - \frac{\partial \tilde{u}\tilde{v}|_h}{\partial y} - \left. \frac{\partial \tilde{p}}{\partial x} \right|_h + \frac{\nu}{h} \left(\left. \frac{\partial \tilde{u}}{\partial z} \right|_h - \eta_0 \right) \right]$$

- Attached-eddy ansatz in overlap region (Townsend, 1976)
 - Hierarchy of streamwise ``attached'' SGS vortices whose size scales with distance from wall
 - Extended stretched-vortex SGS model with attached-eddy assumption
 - SGS model gives log relationship for slip-velocity at lifted wall position $z = h_0$
 - ``Karman constant'' calculated dynamically

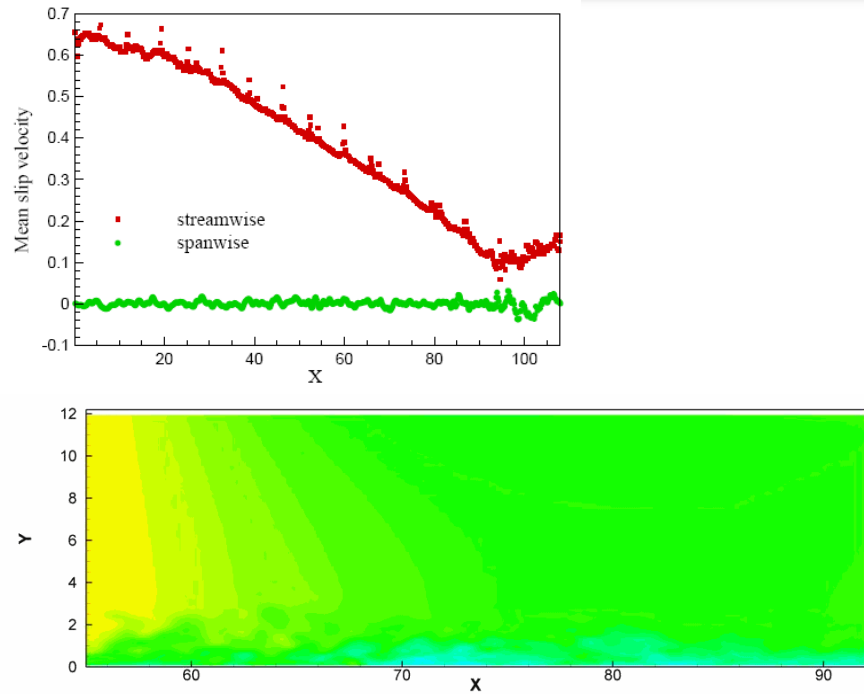
$$\tilde{u}|_{h_0} = u_\tau \left(\frac{1}{\mathcal{K}_1} \log \left(\frac{h_0 u_\tau / \nu}{h_\nu^+} \right) + h_\nu^+ \right) \quad \mathcal{K}_1 = \frac{\gamma_{II} K^{1/2}}{2 \left(-T_{xz}|_{e_{\bar{S}}} \right)^{1/2}}$$

- Chung & Pullin , JFM (2009)**

Wall model: 2D version



**1D is not sufficient.
We need 2D wall model**



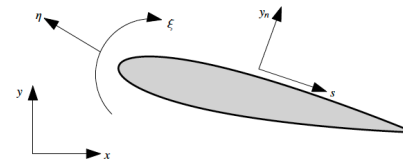
W. Cheng, D. I. Pullin, R. Samtaney. Large-eddy simulation of separation and reattachment of a turbulent boundary layer, *Journal of Fluid Mechanics*, 2015.⁹

Wall model: ODE for Wall Shear Stress and Dirichlet BC for Velocity

- Filtering (wall parallel and top hat in wall normal direction)

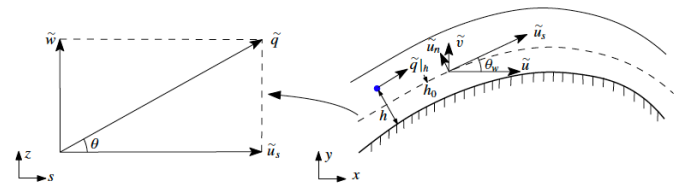
$$\tilde{\phi}(\xi, \eta, \zeta, t) = \iint \phi(\xi, \eta, \zeta, t) G(\xi - \xi', \Delta_f) G(\zeta - \zeta', \Delta_f) d\xi' d\zeta',$$

$$\langle \phi \rangle = \frac{1}{h} \int_0^h \tilde{\phi}(\xi, \eta, \zeta, t) d\eta,$$



- Inner scaling combined with wall normal integration filter

$$\tilde{q}(\xi, \eta, \zeta, t) = u_\tau(\xi, \zeta, t) F(y_n^+), \quad y_n^+ = u_\tau y_n / v,$$



- ODE for wall shear stress

- Terms C_1 and C_2 depend on resolved fields at first mesh point above virtual wall

$$\frac{\partial \eta_0}{\partial t} = C_1 \eta_0 - C_2 \eta_0^2, \quad \frac{\partial \langle q \rangle}{\partial t} = \frac{\tilde{q}|_h}{2\eta_0} \frac{\partial \eta_0}{\partial t},$$

$$\eta_0 \equiv \left. \frac{\partial \tilde{q}}{\partial y_n} \right|_w .$$

- Dirichlet Wall BC

- Similar to Cheng et al. (JFM 2015)

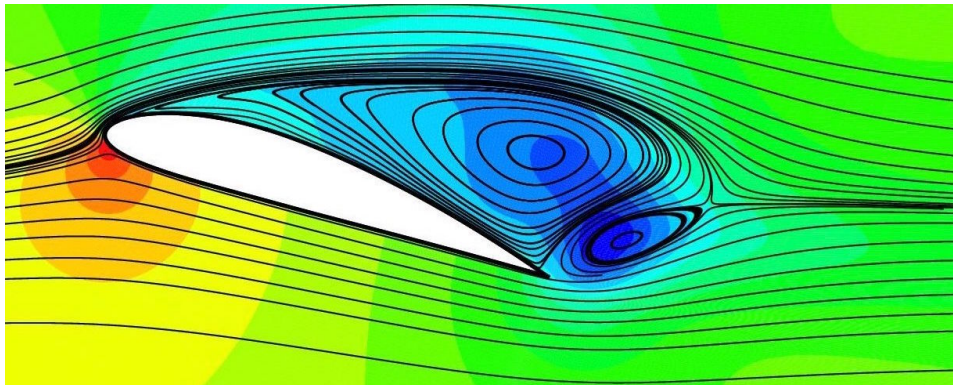
- θ dependence can be taken into account

- θ does not vary from first mesh point to the wall (similar to Cheng et al.)

$$\tilde{q}|_{h_0} = \begin{cases} u_\tau \left(\frac{1}{\mathcal{K}_1} \log \left(\frac{h_0^+}{h_v^+} \right) + h_v^+ \right), & h_0^+ > h_v^+, \\ u_\tau h_0^+, & h_0^+ < h_v^+, \\ u_\tau h_0^+, & \tau_{w,s} \leq 0, \end{cases} \quad \tau_{w,s} > 0,$$

Application 1

Separated Flow Past Airfoils



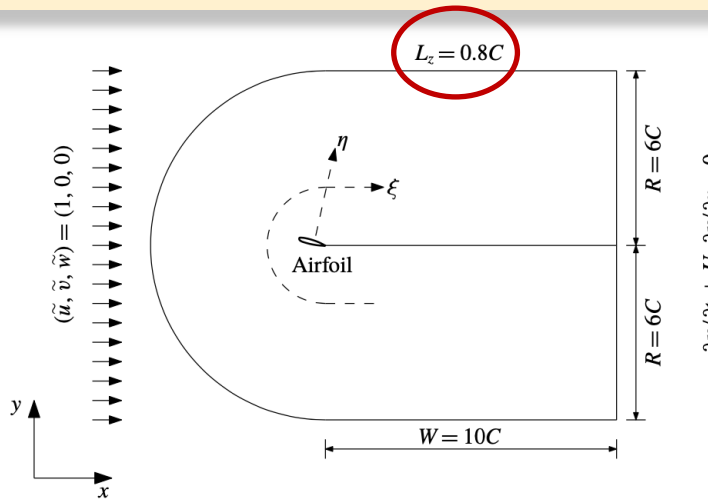
W. Gao, W. Zhang, W. Cheng, R. Samtaney. Wall-modelled large-eddy simulation of turbulent flow past airfoils, *Journal of Fluid Mechanics*, 2019, 873:174-210.

LES of Flow Past an Airfoil: Background

Author	Airfoil	Method	Re_c	AoA	L_z/C (deg.)	Results
Dahlstrom & Davidson (2001)	A-airfoil	WRLES	2.1 M	13.3	0.03	$C_f, C_p, \bar{u}, \overline{u'v'}$
Mary & Sagaut (2002)	A-airfoil	WRLES	2.1 M	13.3	0.012	$C_f, C_p, \bar{u}, \overline{u'v'}$
Morgan & Visbal (2003)	A-airfoil	WRLES	2.1 M	13.3	0.12	$C_f, C_p, \bar{u}, \overline{u'v'}$
Kawai & Asada (2013)	A-airfoil	WMLES	2.1 M	13.3	0.017	$C_f, C_p, \bar{u}, \overline{u'v'}$
Asada & Kawai (2018)	A-airfoil	WRLES	2.1 M	13.3	0.049	$C_f, C_p, \bar{u}, \overline{u'v'}$
George & Lele (2014)	NACA0012	WMLES	1.5 M	6	0.14	$C_p, \bar{u}, \overline{u'v'}$
Asada <i>et al.</i> (2014)	NACA0015	WRLES	1.6 M	20.11	0.05	C_p, \bar{u}
Sato <i>et al.</i> (2016)	NACA0015	WRLES	1.6 M	8.13	0.05	C_L, C_D, C_p, \bar{u}
Schmidt, Franke & Thiele (2001)	NACA4412	WRLES	1.64 M	12	0.05	$C_p, \bar{u}, \overline{u'v'}$
Bose & Moin (2014)	NACA4412	WMLES	1.6 M	13.8	0.1	C_p, \bar{u}
Park & Moin (2014)	NACA4412	WMLES	1.64 M	12	0.72	C_p, \bar{u}

TABLE 1. Summary of LES performed in flow past an airfoil at high Re_c . Here suffix 'M' refers to million; \bar{u} denotes the velocity, $\overline{u'v'}$ refers to the Reynolds stress tensor components, C_p is the pressure coefficient, C_f is the skin-friction coefficient and L_z/C is the ratio of the spanwise domain size to chord length.

Numerical Setup



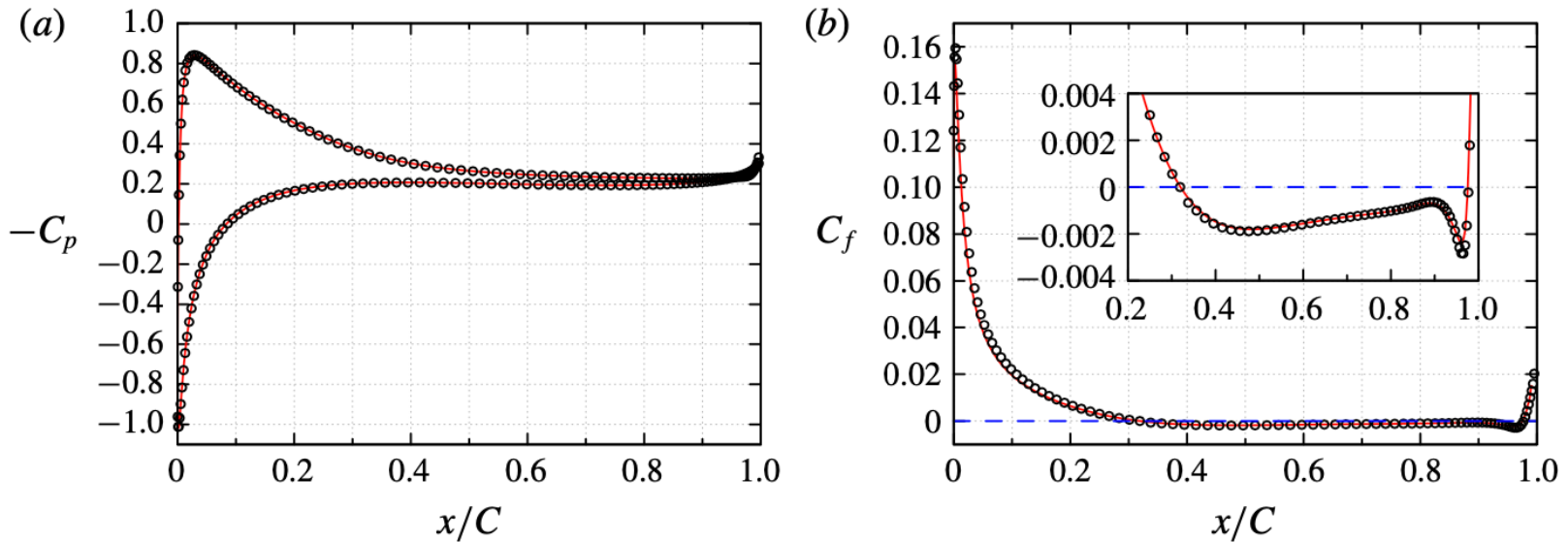
**All model
“parameters”
held fixed for
all cases.**

No “tweaking”

Airfoil	Method	Re_c	AoA (deg.)	$N_\xi \times N_\eta \times N_z$	$\Delta\xi_{max}^+$	$\Delta\eta_{max}^+$	Δz_{max}^+
NACA0012	DNS	10^4	5	$2048 \times 256 \times 256$	7.4	0.8	8.8
NACA0012	WMLES	10^4	5	$768 \times 96 \times 64$	19.7	14.2	38.4
NACA0018	WMLES	10^5	5	$1600 \times 128 \times 128$	54.9	15.8	65.8
A-Airfoil	WMLES	2.1×10^6	13.3	$3200 \times 256 \times 256$	80.1	16.4	85.4

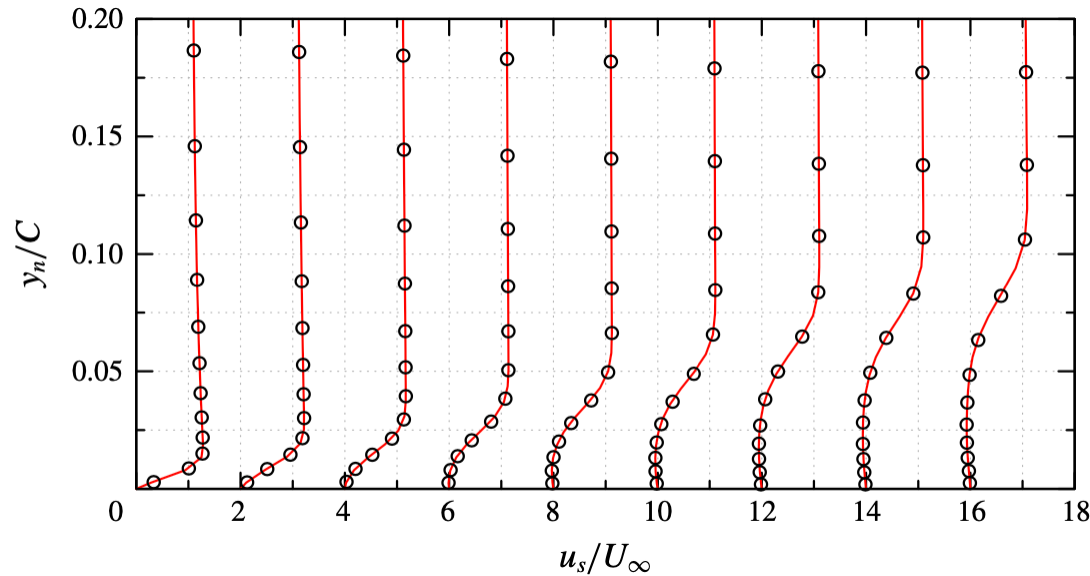
TABLE 2. Summary of the performed numerical cases.

NACA0012, $Re_c=10^4$: C_p and C_f



Circles: WMLES; Lines: DNS

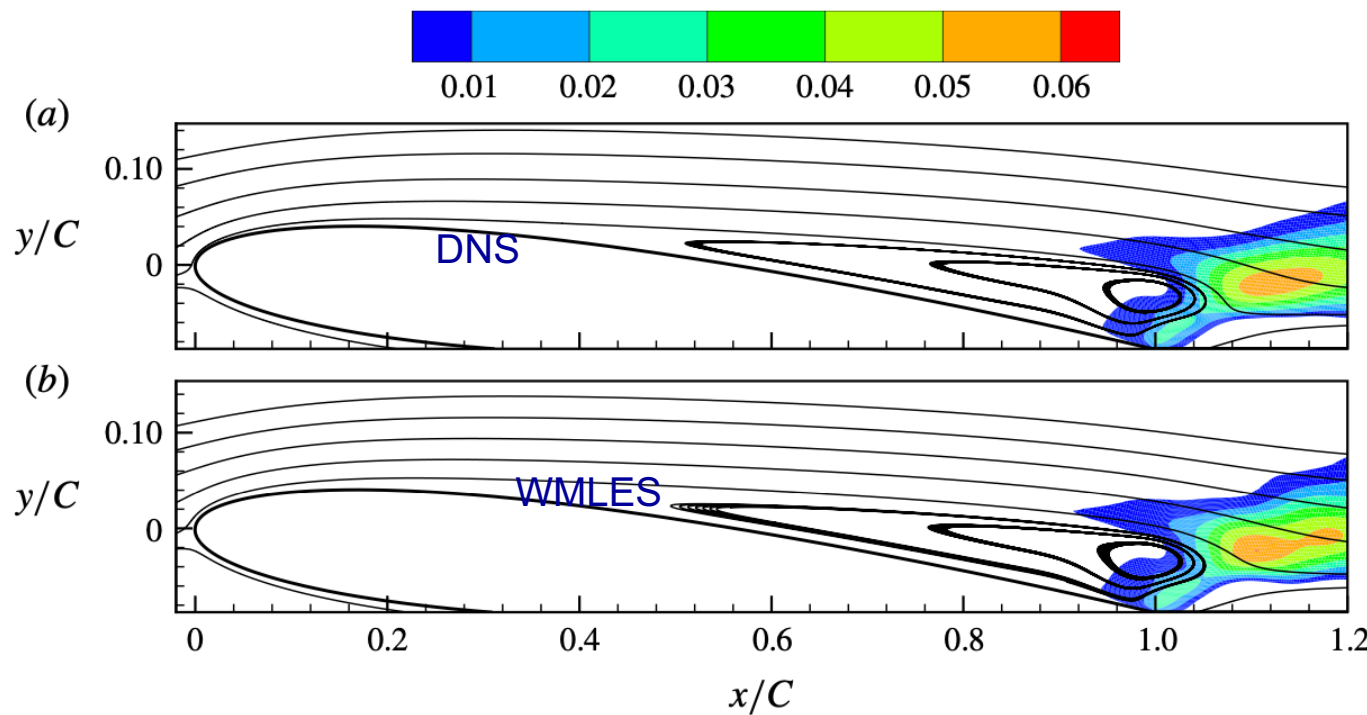
NACA0012, $Re_c=10^4$: u_s



$x/C=[0.1,0.9]$ with equal distance 0.1

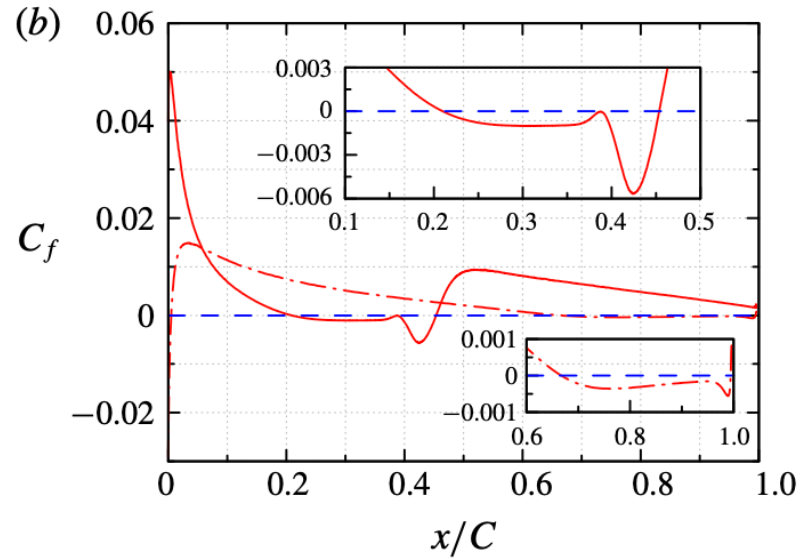
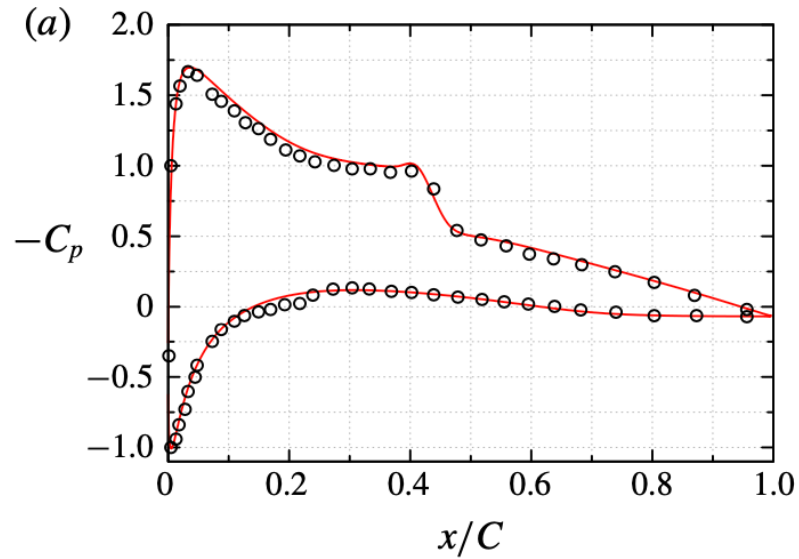
Circles: DNS; Lines: WMLES

NACA0012, $Re_c=10^4$: $-\overline{u'v'}$



$$-\overline{u'v'}/U_\infty^2 = [-0.001, 0.06]$$

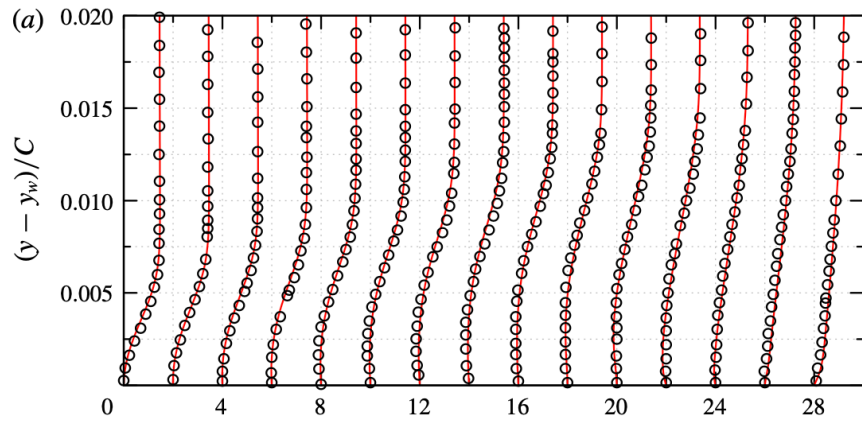
NACA0018, $Re_c=10^5$: C_p and C_f



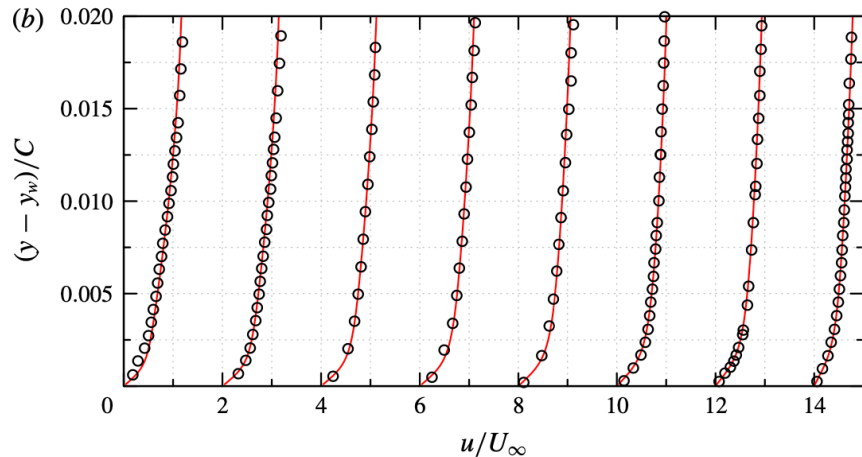
Circles: experimental data from Kirk & Yarusevych (2017)
 $x_s/C = 0.24 \pm 0.02, x_r/C = 0.52 \pm 0.02$
 $x_s/C = 0.21, x_r/C = 0.45$

Red solid lines: WMLES

NACA0018, $Re_c=10^5$: u

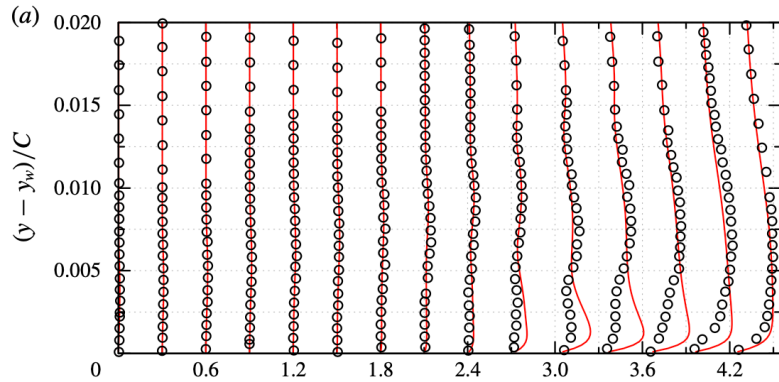


$x/C=[0.2, 0.48]$ with
equal distance 0.02

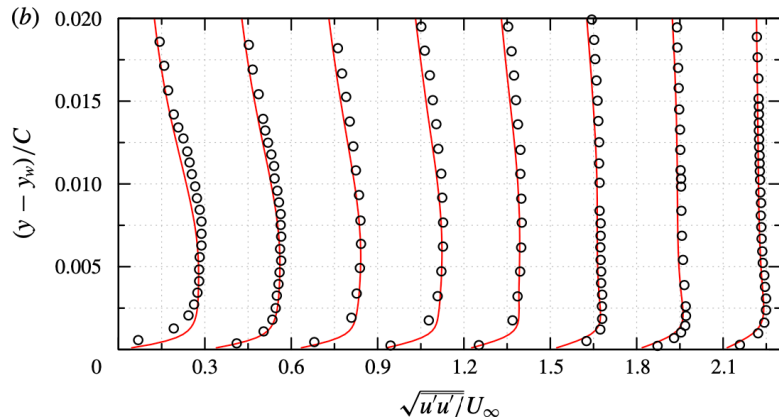


$x/C=0.50, 0.52, 0.54,$
 $0.56, 0.60, 0.66,$
 $0.73, 0.87$

NACA0018, $Re_c=10^5$: $\sqrt{u'u'}/U_\infty$

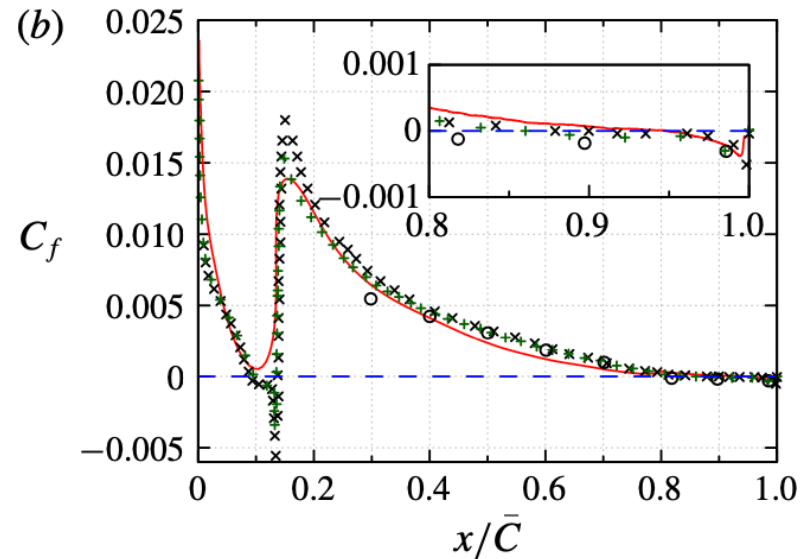
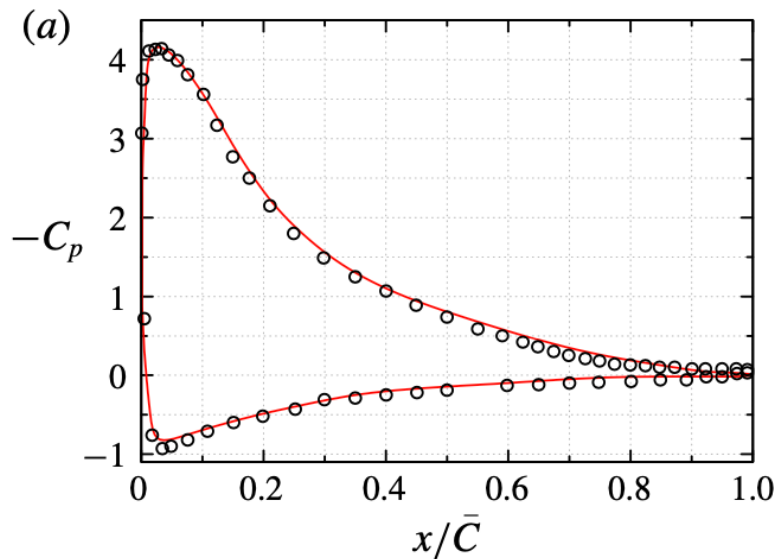


$x/C=[0.2,0.48]$ with
equal distance 0.02



$x/C=0.50, 0.52, 0.54,$
 $0.56, 0.60, 0.66,$
 $0.73, 0.87$

Aérospatiale A-airfoil, $Re_c=2.1\times 10^6$: C_p and C_f



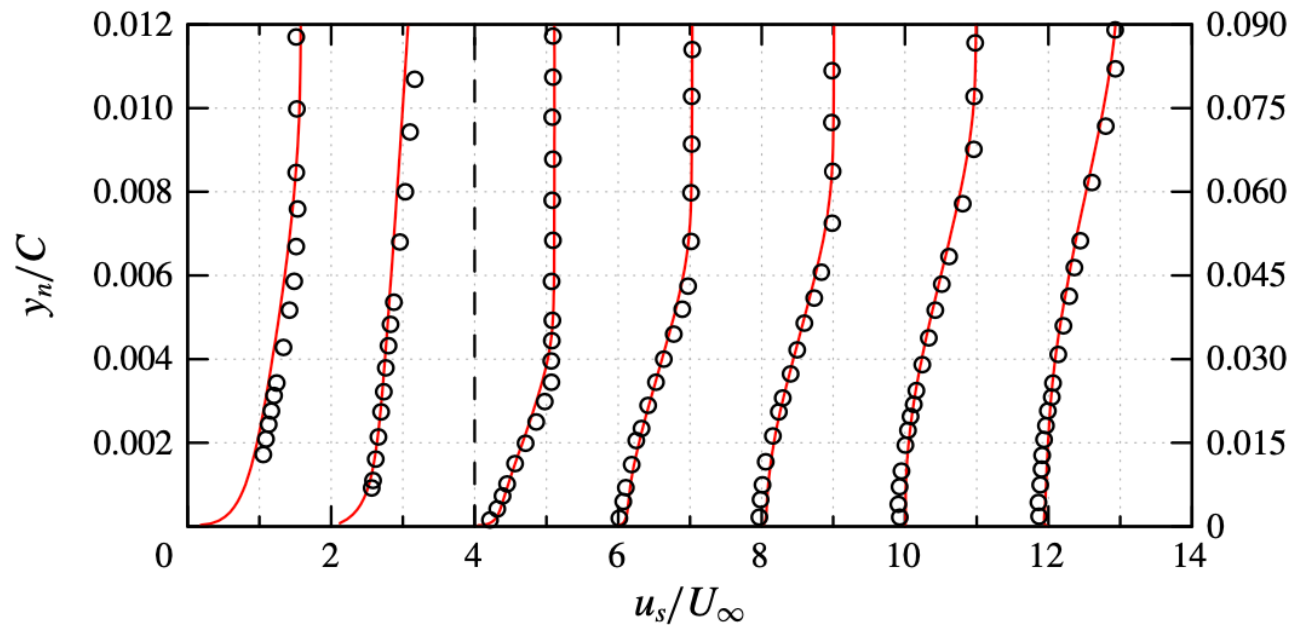
Circles: experimental data from Gleyzes (1988), $x_s/C \approx 0.82$

Cross: WRLES from Mary & Sagaut (2002)

Plus: WRLES from Asada & Kawai (2018)

Lines: WMLES, $x_s/C = 0.9$

Aérospatiale A-airfoil, $Re_c=2.1\times 10^6$: u_s

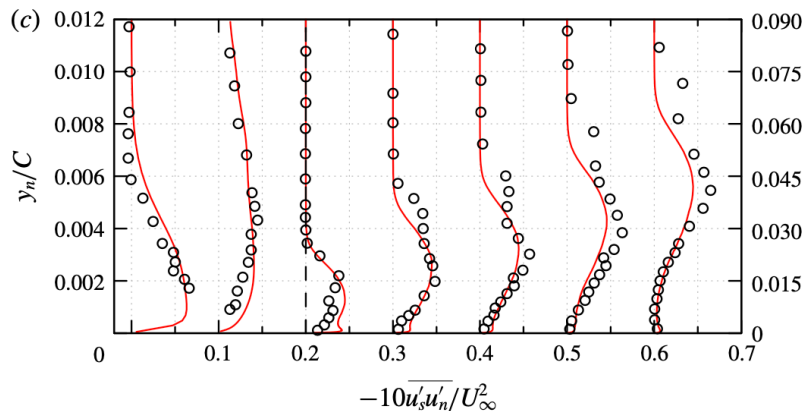
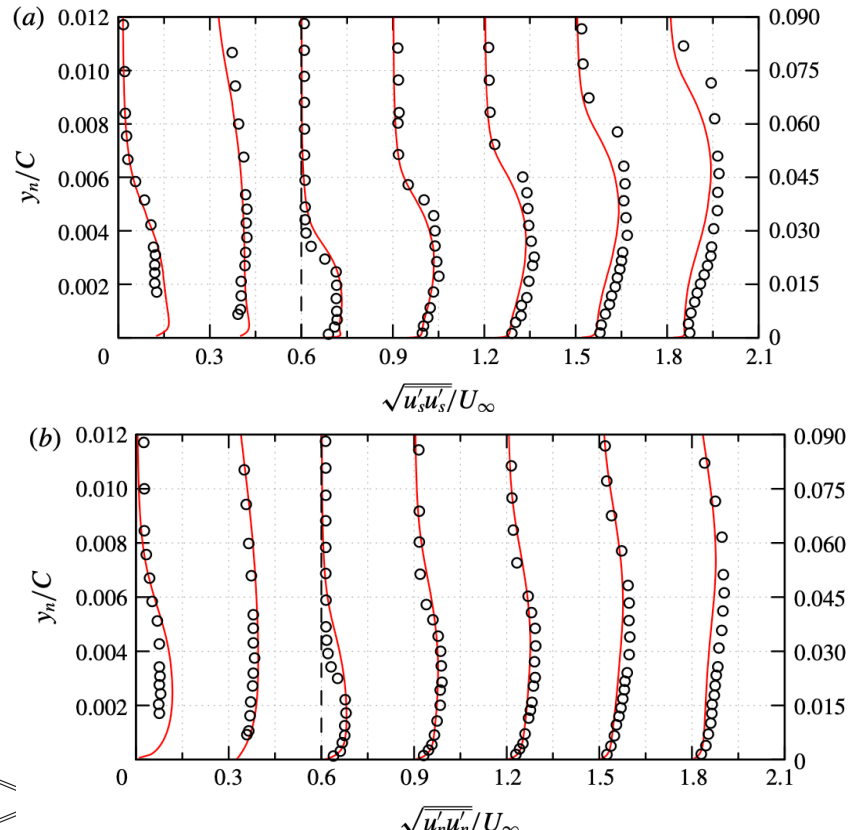


Circles: experimental data from Gleyzes (1988)

Lines: WMLES

$x/C = 0.3, 0.5, 0.7, 0.825, 0.87, 0.93, 0.99$.

Aérospatiale A-airfoil, $Re_c=2.1\times 10^6$: $\overline{u'_i u'_j}$



Anisotropy of the Flow: Lumley Triangle

Anisotropy tensor: $b_{ij} = \overline{u'_i u'_j} / \overline{u'_k u'_k} - \delta_{ij}/3$ characterized by two invariants (Lumley 1978, Choi & Lumley 2001):

$$II = -b_{ij}b_{ij}/2, \quad III = b_{ij}b_{jk}b_{ki}/3$$

Anisotropy invariant map (AIM): (ϕ, ψ) -Plane

$$\phi = \left(\frac{III}{2} \right)^{1/3}, \quad \psi = \left(-\frac{II}{3} \right)^{1/2}$$

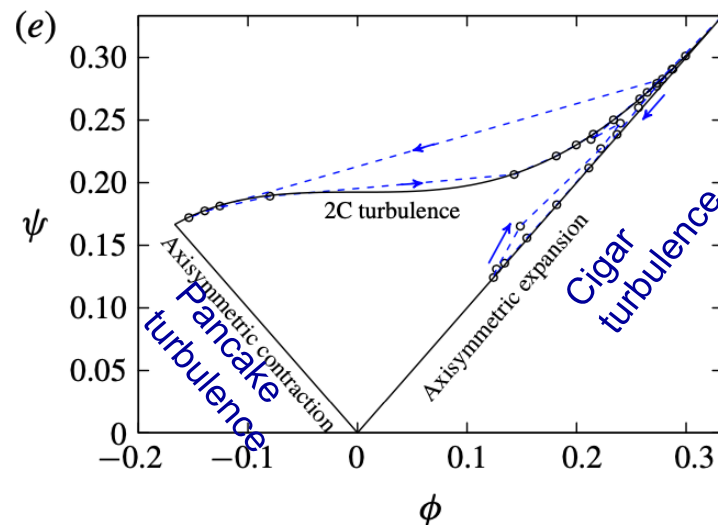
(0, 0): 3D isotropic turbulence

(-1/6, 1/6): two-component (2C)

isotropic turbulence

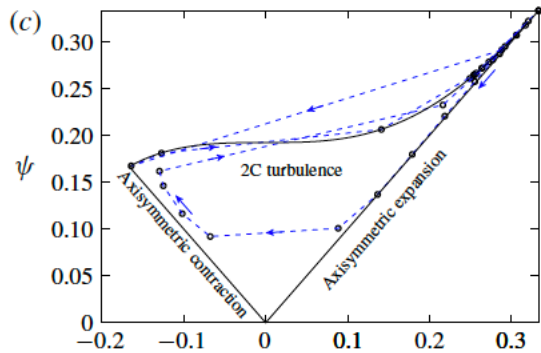
(1/3, 1/3): one-component turbulence

Realizability condition: all states must lie within Lumley Triangle

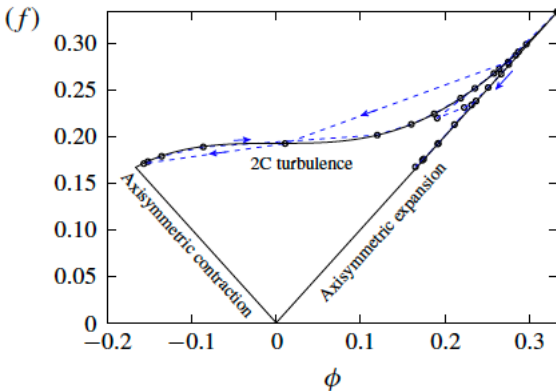


Anisotropy of the Flow: NACA0012, $Re_c=10^4$

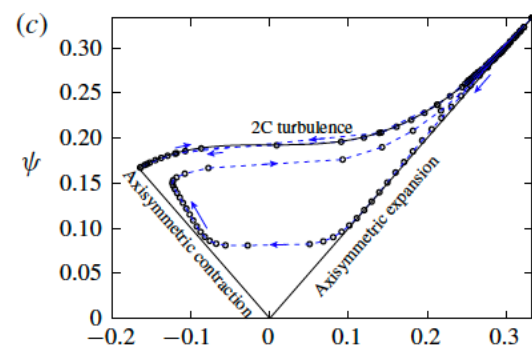
$x/C = 0.92$



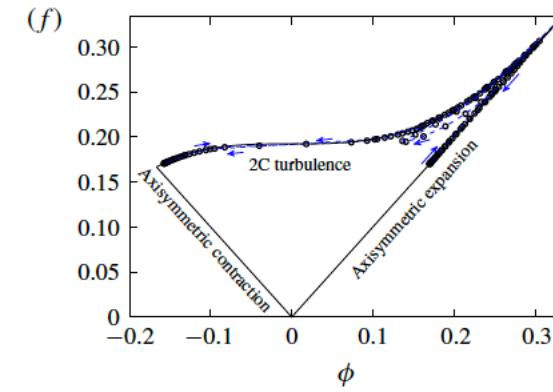
$x/C = 0.98$



WMLES

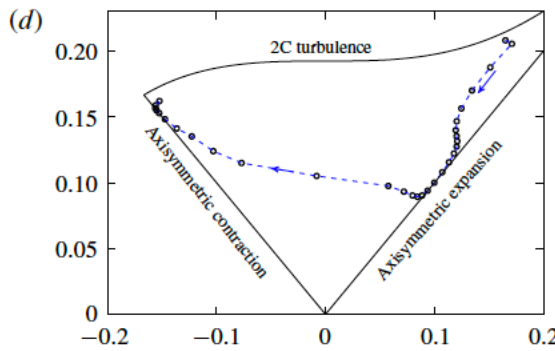


DNS

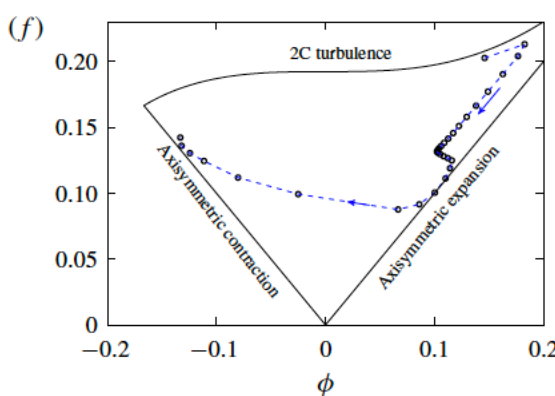


34

Anisotropy of the Flow: NACA0018, $Re_c=10^5$

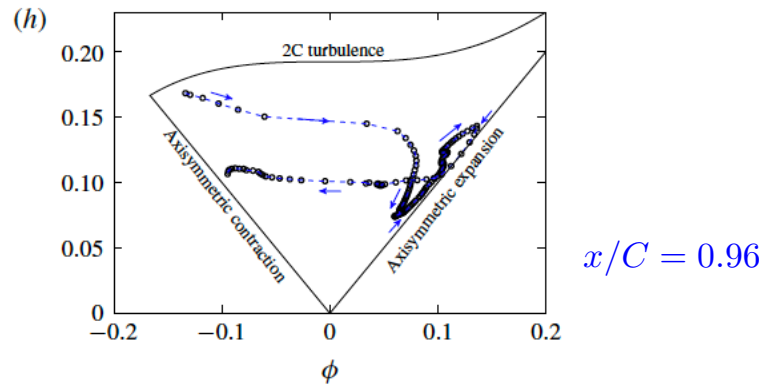
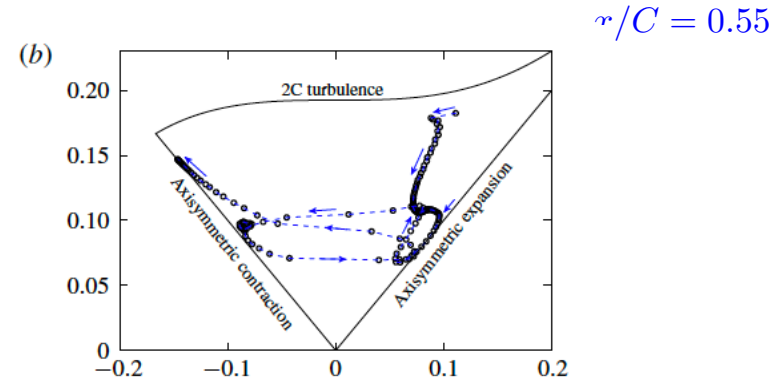


$x/C = 0.65$

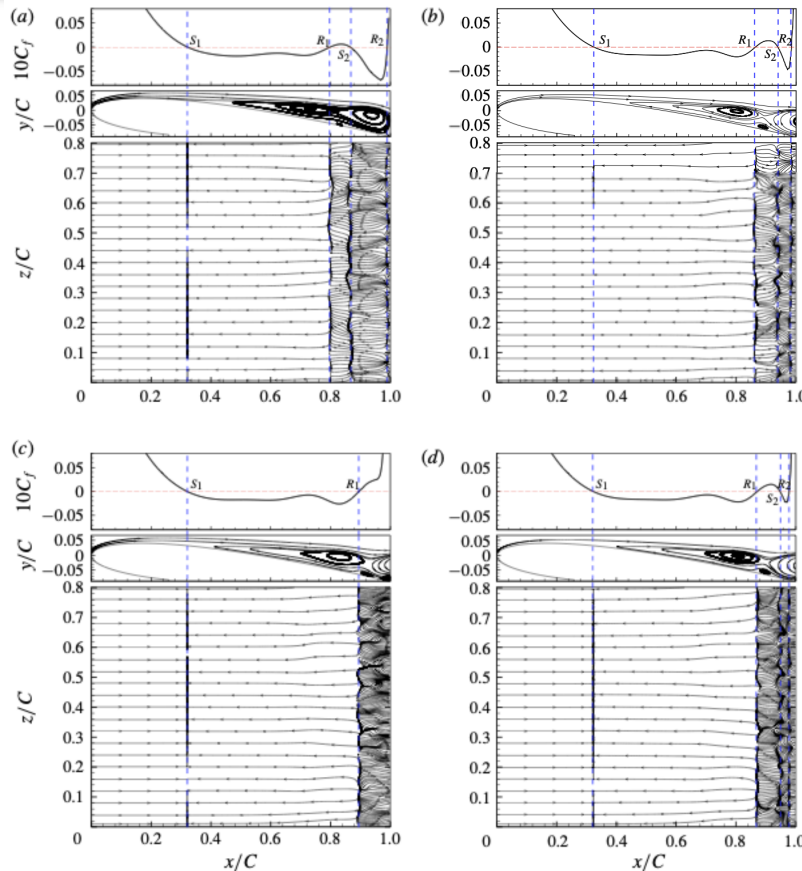


$x/C = 0.95$

Anisotropy of the Flow: A-airfoil, $Re_c=2.1\times 10^6$



Unsteady Flow Separation and Reattachment



NACA0012

$Re_c=10^4$

$tU_\infty/C =$

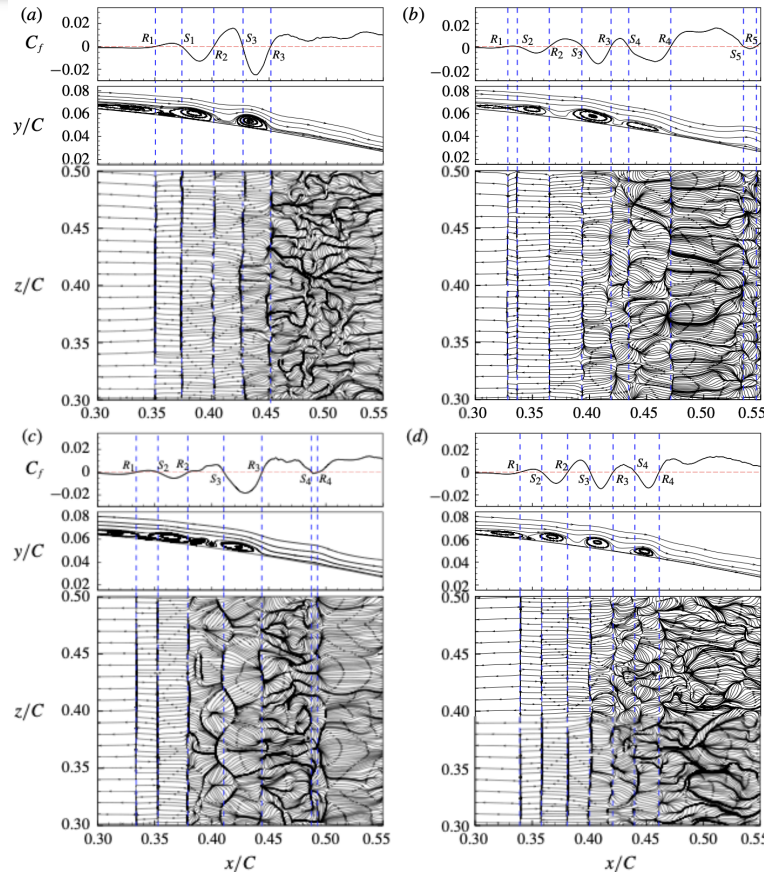
(a) 80.21

(b) 82.16

(c) 83.72

(d) 85.22

Unsteady Flow Separation and Reattachment



NACA0018

$Re_c = 10^5$

$tU_\infty/C =$

(a) 57.59

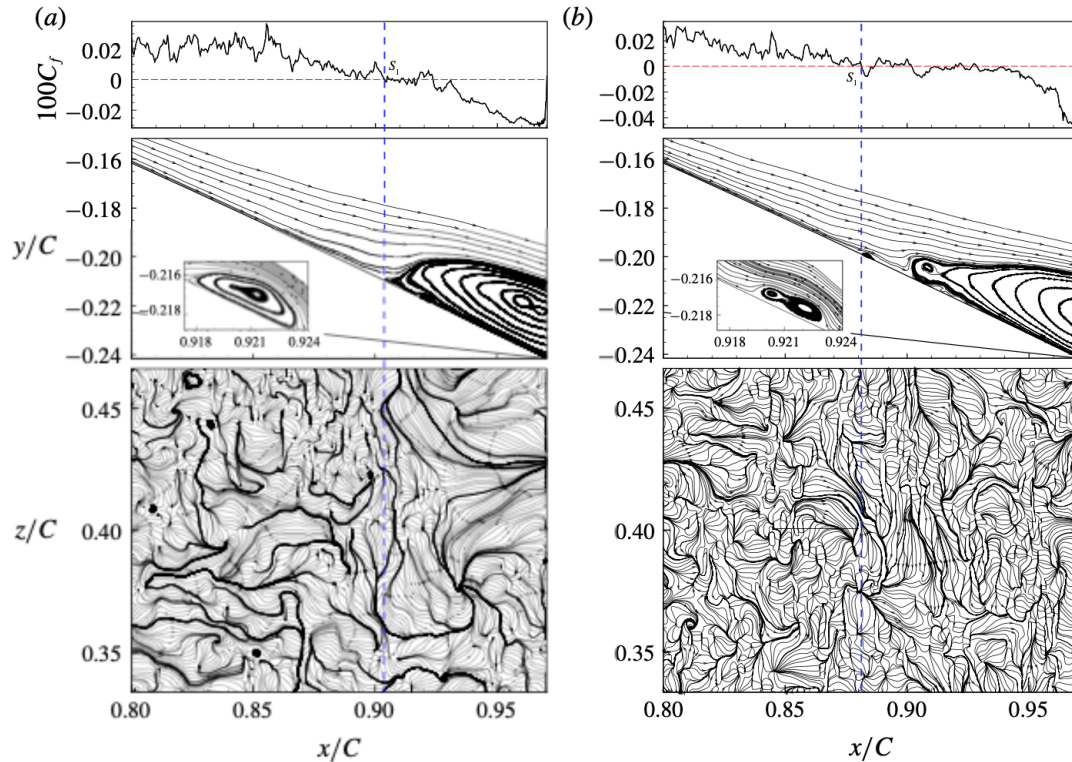
(b) 57.74

(c) 58.49

(d) 59.13

$x_s/C = 0.21, x_r/C = 0.45$

Unsteady Flow Separation and Reattachment



A-airfoil

$$Re_c = 2.1 \times 10^6$$

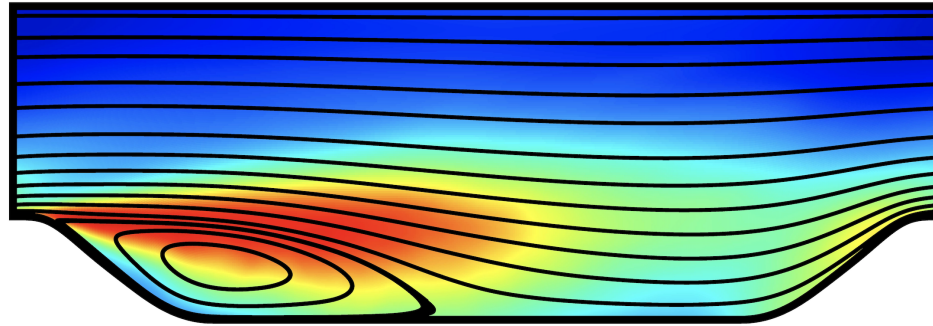
$$tU_\infty/C =$$

(a) 15.92

(b) 16.91

Application 2

Turbulent Flows in a Periodic Hill Channel

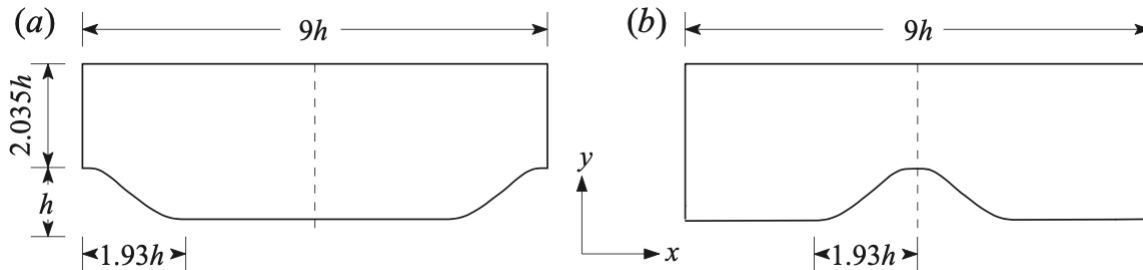


W. Gao, W. Cheng, R. Samtaney. Large-eddy simulations of turbulent flow in a channel with streamwise periodic constrictions, *Journal of Fluid Mechanics*, 2020, to appear.

Numerical Setup

All model
“parameters”
held fixed for
all cases
and same
as the airfoil
simulations

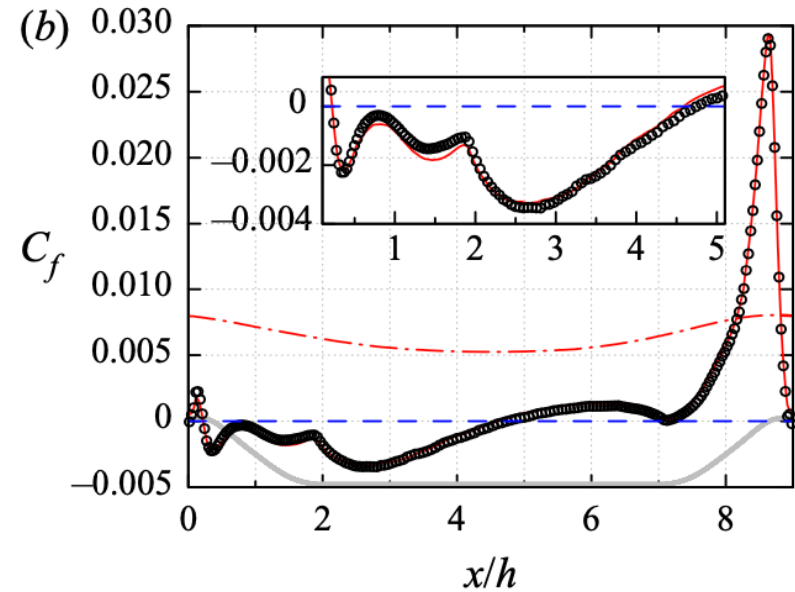
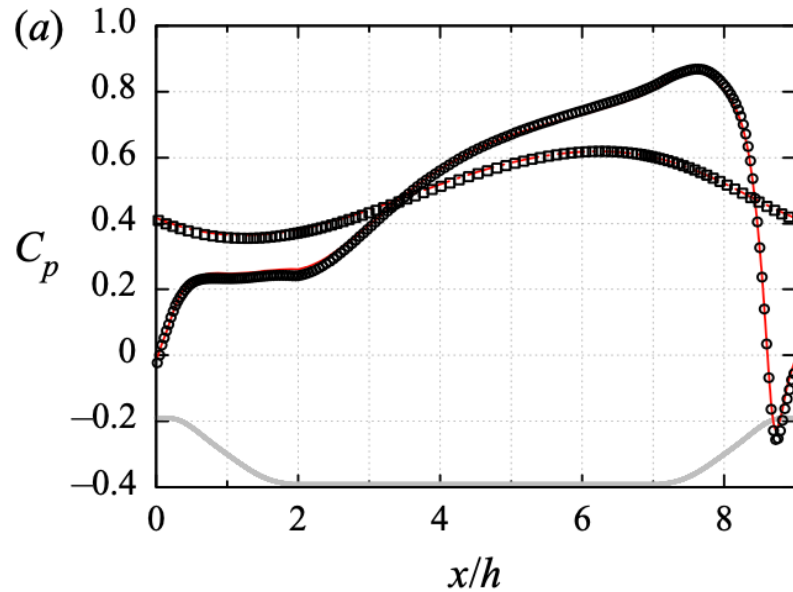
No “tweaking”



Case	Method	Re_h	$N_\xi \times N_\eta \times N_z$	$\Delta\eta_{(b,t)}^+$	$\Delta\xi^+/\Delta\eta_{(b,t)}^+$	$\Delta z^+/\Delta\eta_{(b,t)}^+$	t_a/t_r
M1	WMLES	10 595	$128 \times 64 \times 64$	(19.3, 13.4)	(5.1, 3.5)	(4.7, 3.5)	60
M2	WMLES	33 000	$384 \times 128 \times 128$	(16.1, 15.2)	(5.1, 2.6)	(7.0, 3.9)	46
R2	WRLES	33 000	$1280 \times 256 \times 256$	(0.97, 0.85)	(25.5, 14.1)	(58.6, 35.2)	30
M3	WMLES	10^5	$960 \times 256 \times 256$	(18.0, 15.9)	(4.1, 2.3)	(7.0, 4.4)	40

TABLE 1. Summary of the performed numerical cases. The ‘+’ superscript indicates the expression of the mesh quantities using wall units and the subscripts ‘ b ’ and ‘ t ’ denote the bottom and top walls, respectively. Time $t_r = 9h/U_b$ is the typical flow-through time and t_a is the total simulation time.

$Re_h=10595$: C_p and C_f

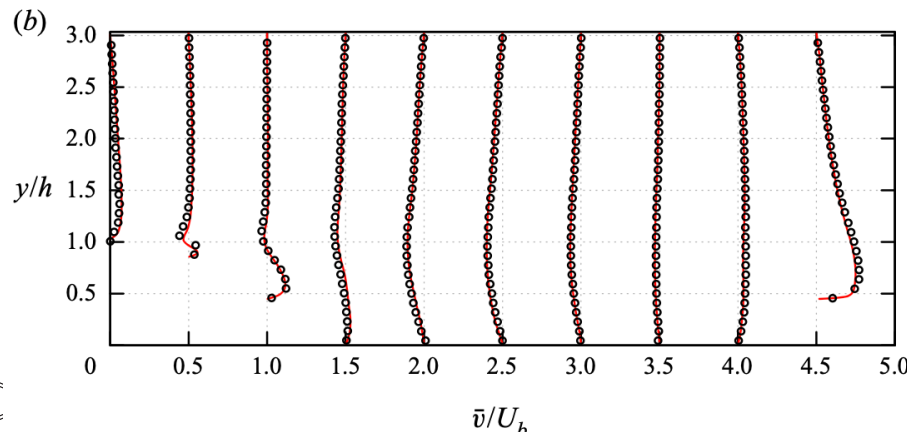
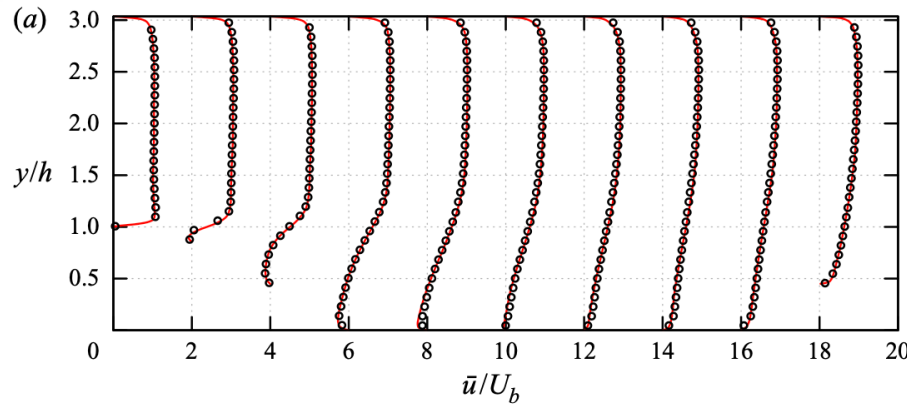


Circles: bottom wall; Square: top wall, WRLES by Fröhlich *et al.* (2005)

Lines: WMLES

$x_s/h=0.22$ $x_t/h=4.6$ (4.21 in expt by Rapp&Manhart, 2011)

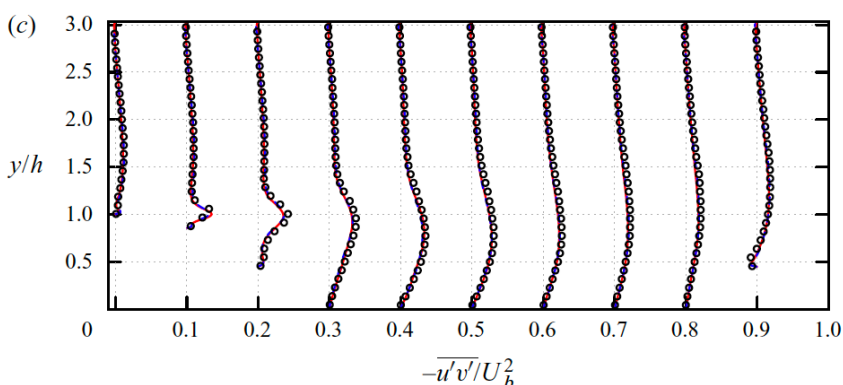
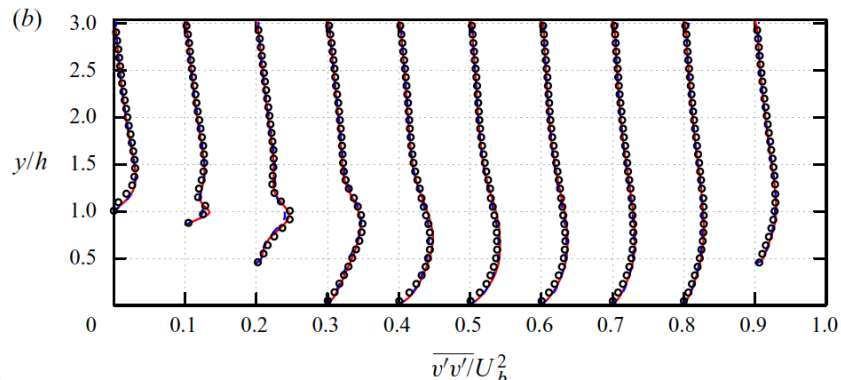
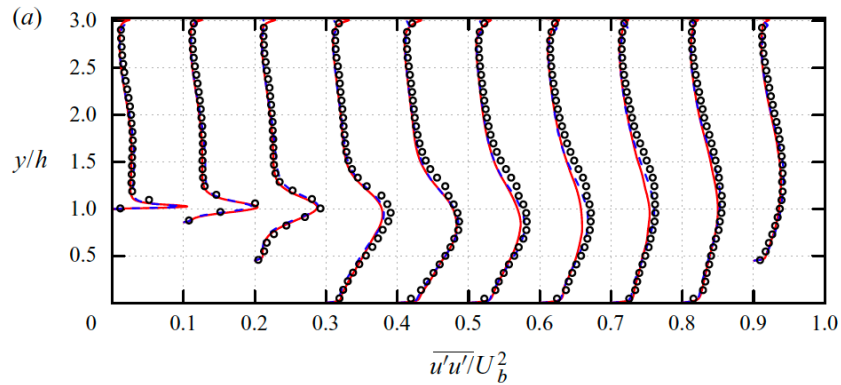
$Re_h=10595$: Mean Velocity Profiles



Circles: experiment by
Rapp & Manhart (2011)
Lines: WMLES

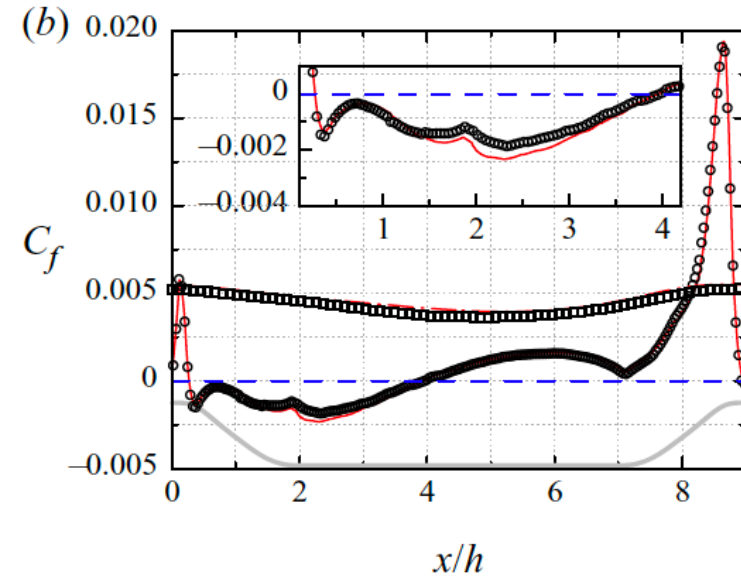
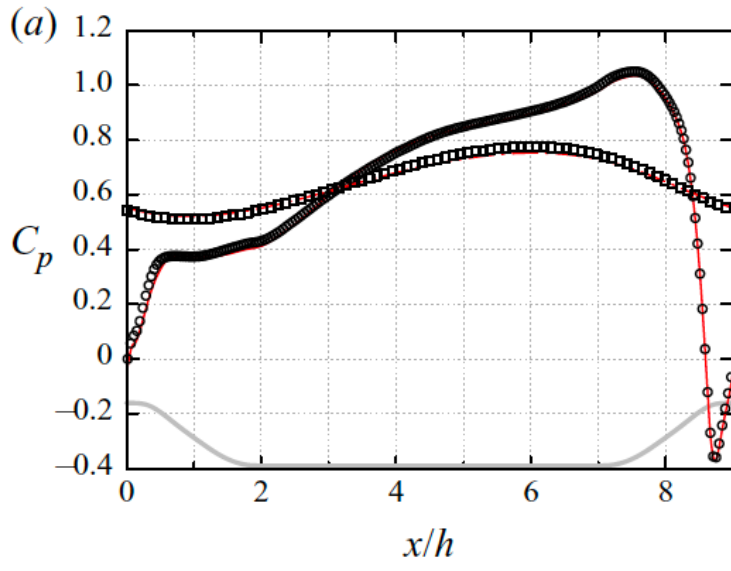
Monitor lines are at $x/h =$
0.05, 0.5, 1, 2, 3, 4, 5, 6, 7, 8

$Re_h=10595$: Reynolds Stress



Circles: experiment by
Rapp & Manhart (2011)
Dashed lines: WRLES by
Fröhlich *et al.* (2005)
Solid red lines: WMLES

$Re_h=33000$: C_p and C_f

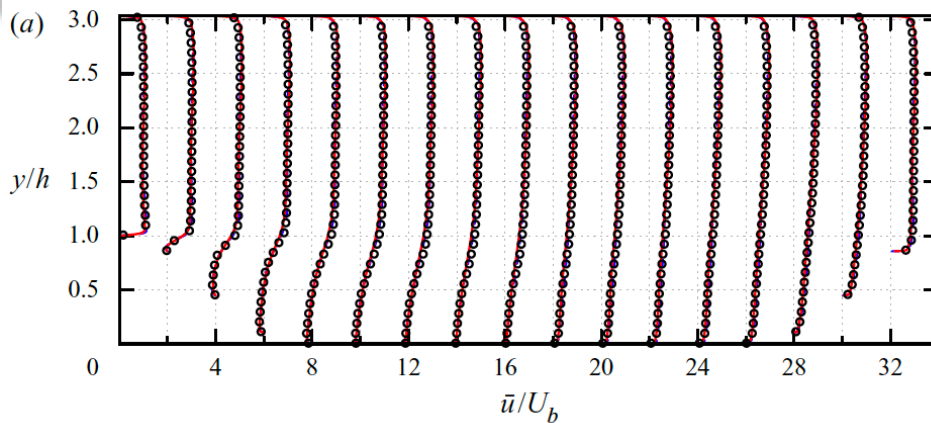


Circles: bottom wall; Square: top wall, WRLES

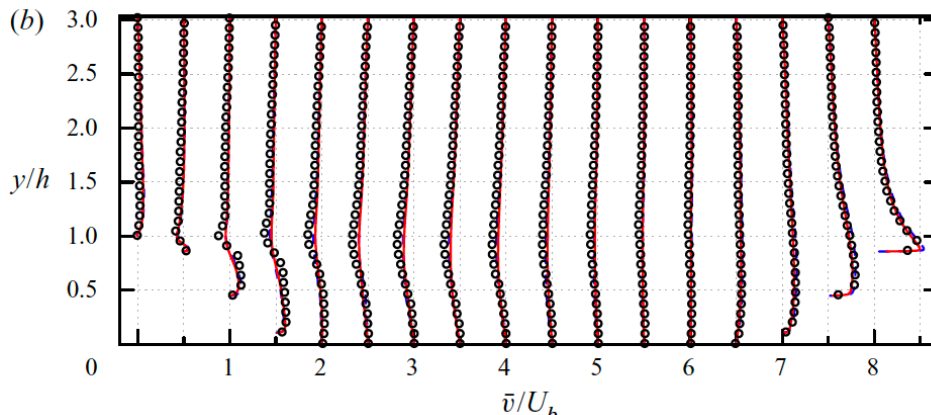
Lines: WMLES

$x_s/h=0.27$ $x_t/h = 3.94$ (0.34 ± 0.05 , 3.80 ± 0.05 expt by Kähler et al. 2016)⁴⁵

$Re_h=33000$: Mean Velocity Profiles

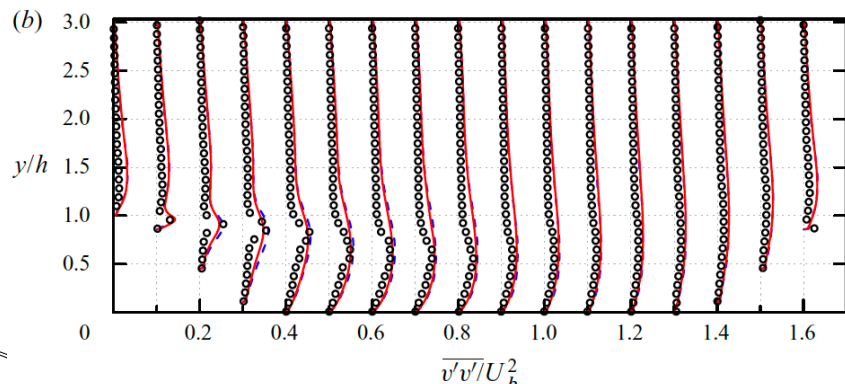
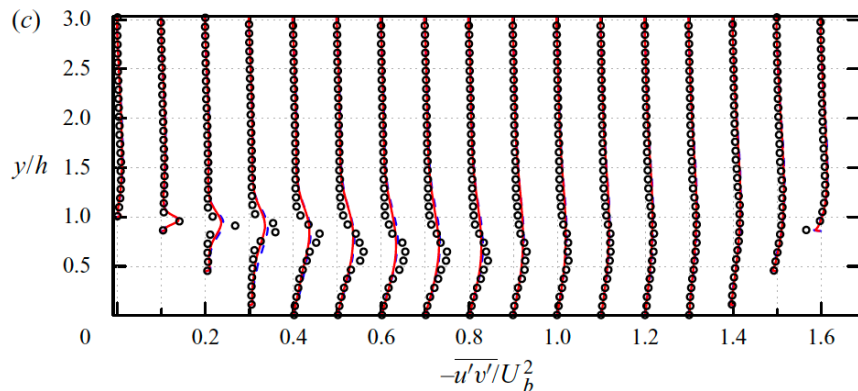
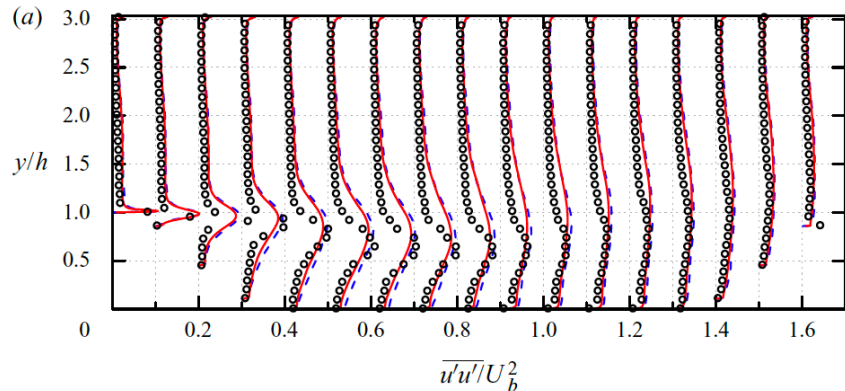


Circles: experiment by
Kähler et al. (2016)
Lines: WMLES



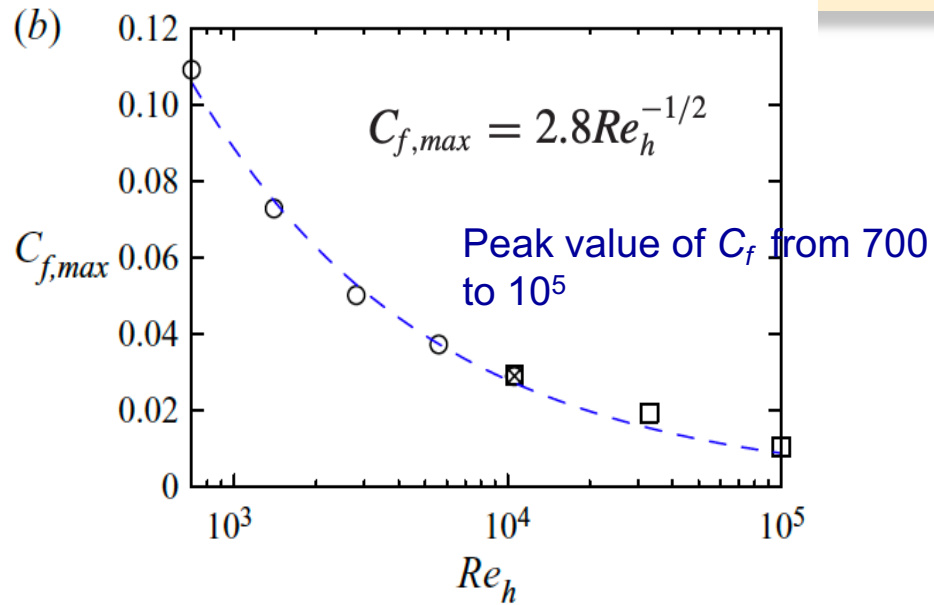
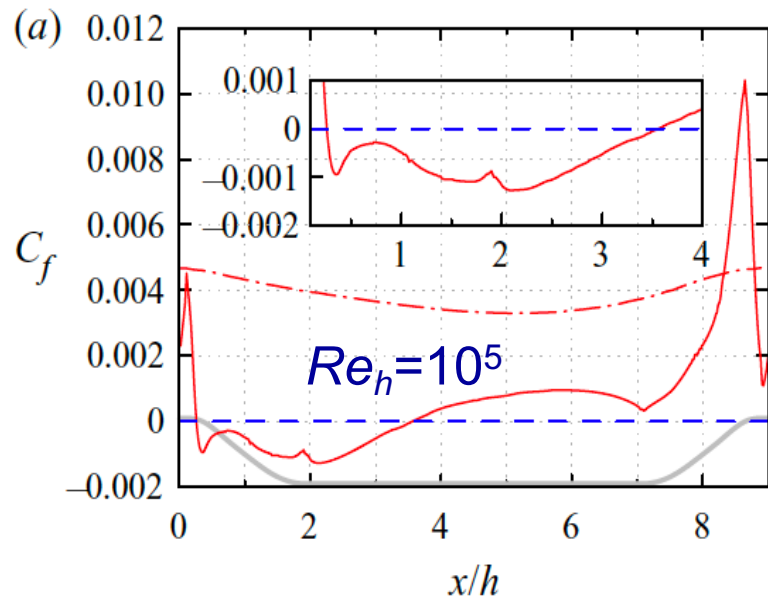
Monitor lines are at $x/h = [0, 9]$ with equal gap 0.5

$Re_h=33000$: Reynolds Stress



Circles: experiment by
Kähler et al. (2016)
Dashed lines: WRLES
Solid red lines: WMLES

Reynolds Number Effects and Peak Skin Friction

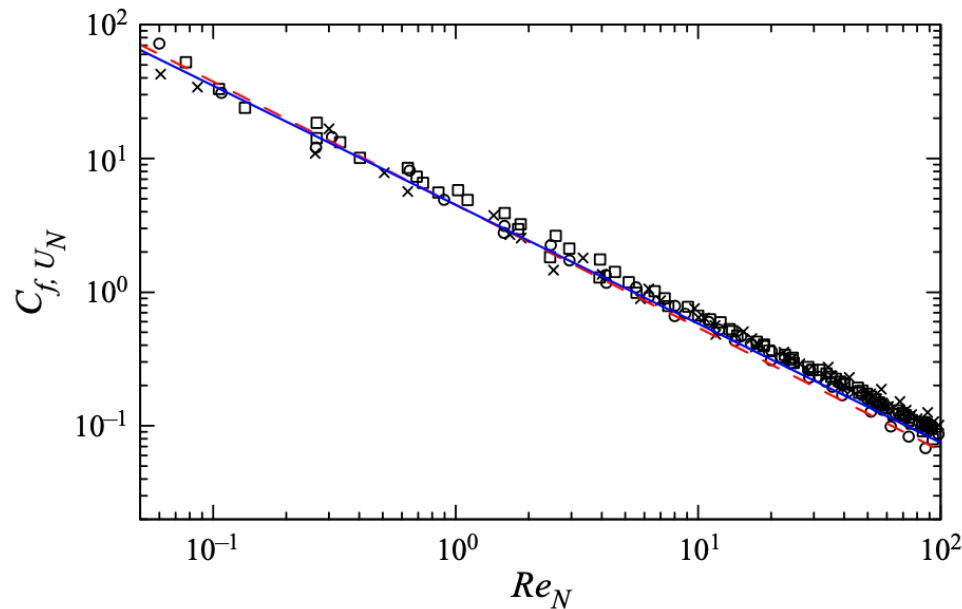


Circles: DNS/WRLES from Breuer *et al.* (2009)

Cross: WRLES from Fröhlich *et al.* (2005)

Squares: WMLES

Skin Friction Inside the Separation Zone



Circles: $Re_h=10595$; Squares: $Re_h=33000$; Cross: $Re_h=10^5$

Dashed line: $C_{f,U_N} \approx 4.5Re_N^{-0.92}$ by Le, Moin & Kim (1997)

Solid line: $C_{f,U_N} \approx 4.5Re_N^{-0.89}$

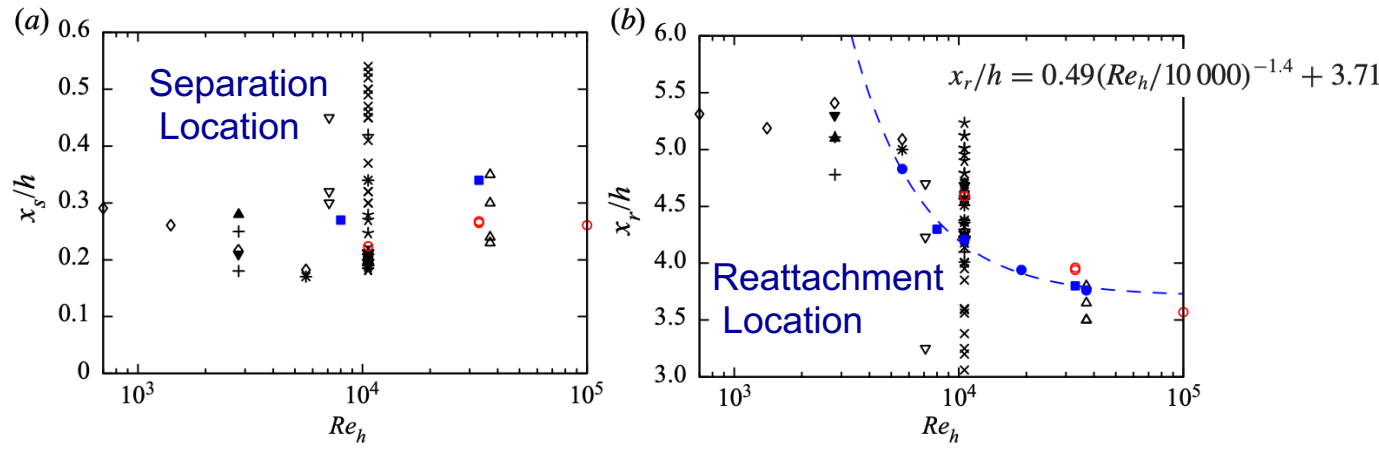
$$C_{f,U_N} = 2|\tau_{w,s}|/\rho U_N^2$$

$$Re_N = U_N N / \nu$$

U_N : maximum back-flow velocity

N : distance of U_N away from the wall

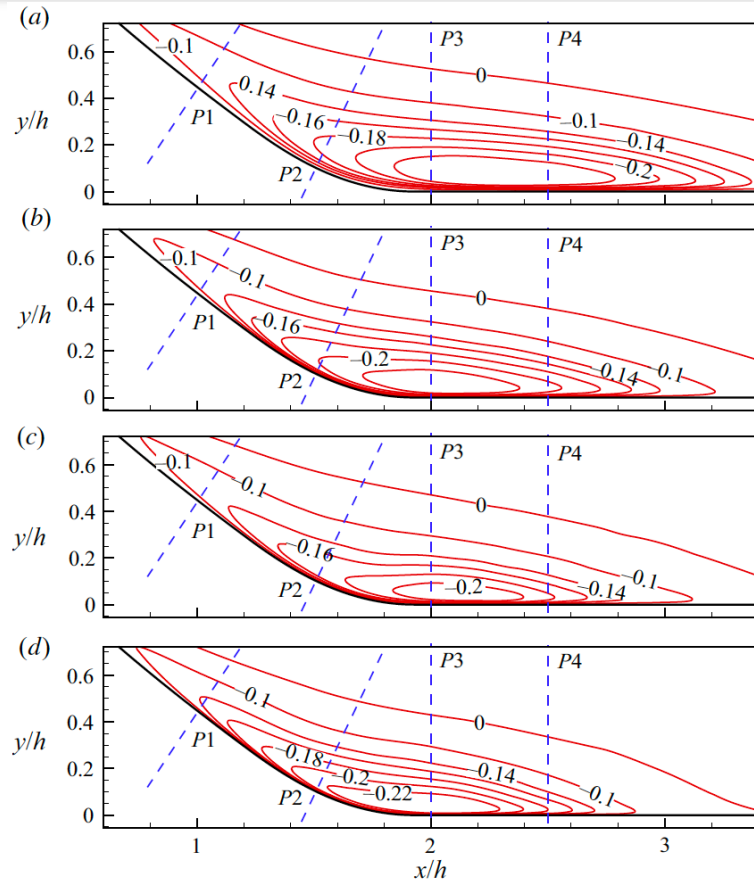
Reynolds Number Effects: Separation/Reattachment Locations and Bubble Centroid/Size



Case	Re_h	x_c/h	y_c/h	L_b/h	H_b/h
M1	10 595	2.01	0.53	4.37	0.91
Fröhlich <i>et al.</i> (2005)	10 595	2.07	0.53	4.40	0.93
M2	33 000	1.87	0.48	3.67	0.83
R2	33 000	1.88	0.49	3.69	0.82
Kähler <i>et al.</i> (2016)	33 000	2.05 ± 0.1	0.48 ± 0.02	3.46 ± 0.1	0.82
M3	10^5	1.82	0.46	3.31	0.80

TABLE 2. Comparison of bubble size with experimental and LES results: centre coordinate of the recirculation zone (x_c, y_c), length of the bubble (L_b) and height of the bubble (H_b).

Scaling of Streamwise Velocity Profiles in the Separation Zone



$Re_h = 10595$

WMLES

$Re_h = 33000$

WMLES

$Re_h = 33000$

WRLES

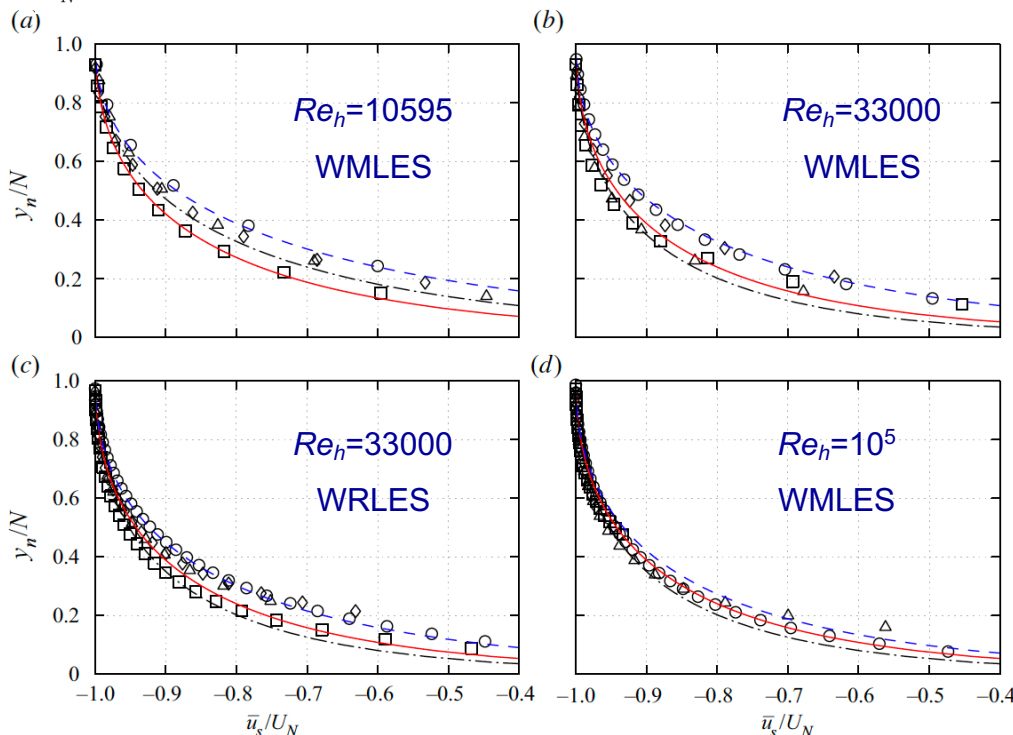
$Re_h = 10^5$

WMLES

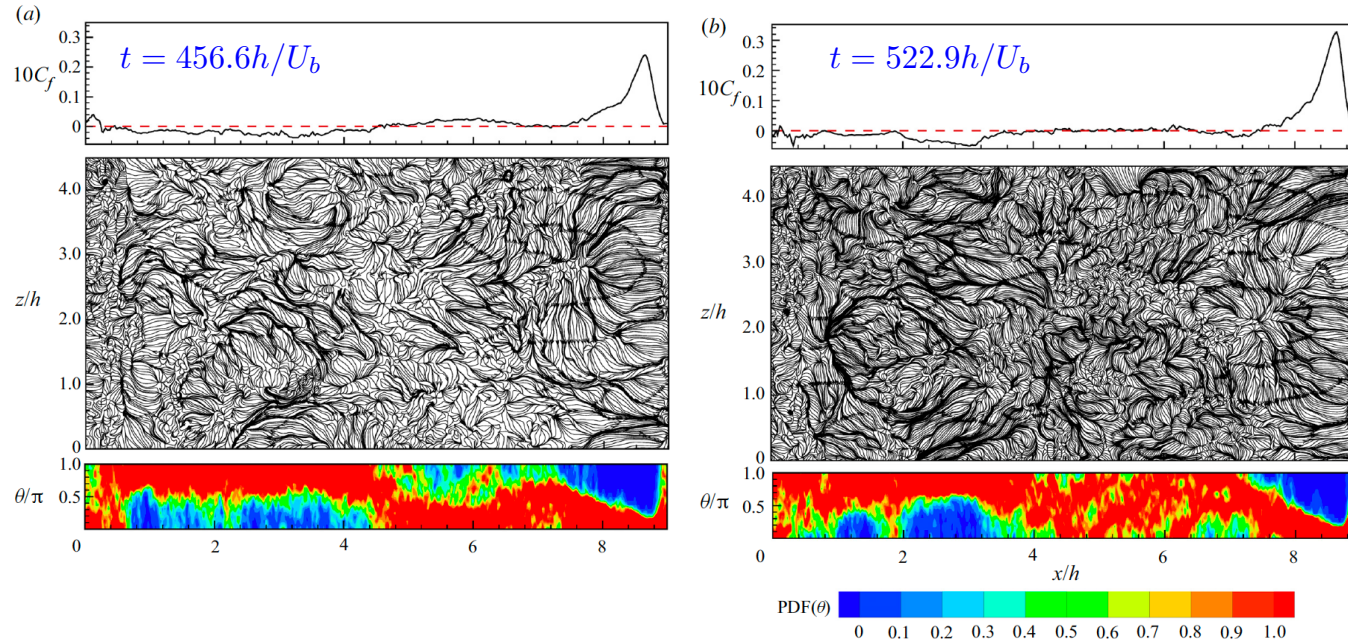
Scaling of Streamwise Velocity Profiles in the Separation Zone

$$\frac{\bar{u}_s}{U_N} = A \left(\frac{y_n}{N} - \ln \left| \frac{y_n}{N} \right| - 1 \right) - 1$$

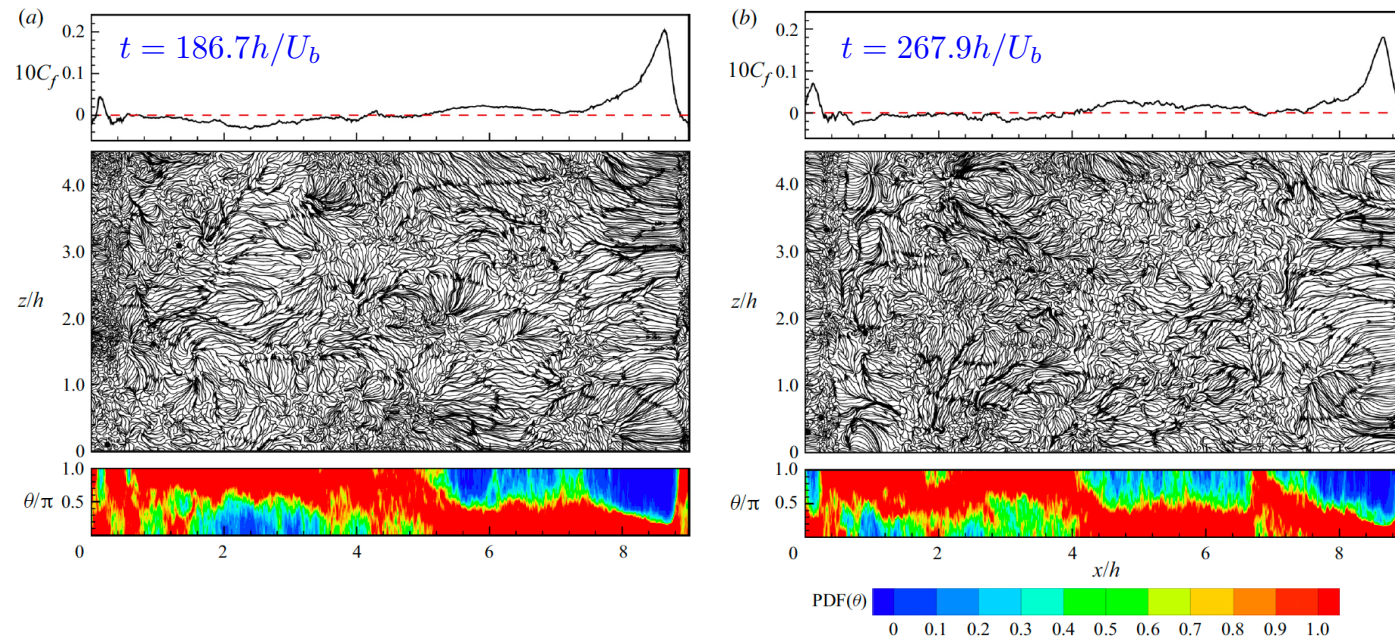
$A=0.3$: solid lines, Simpson (1983)



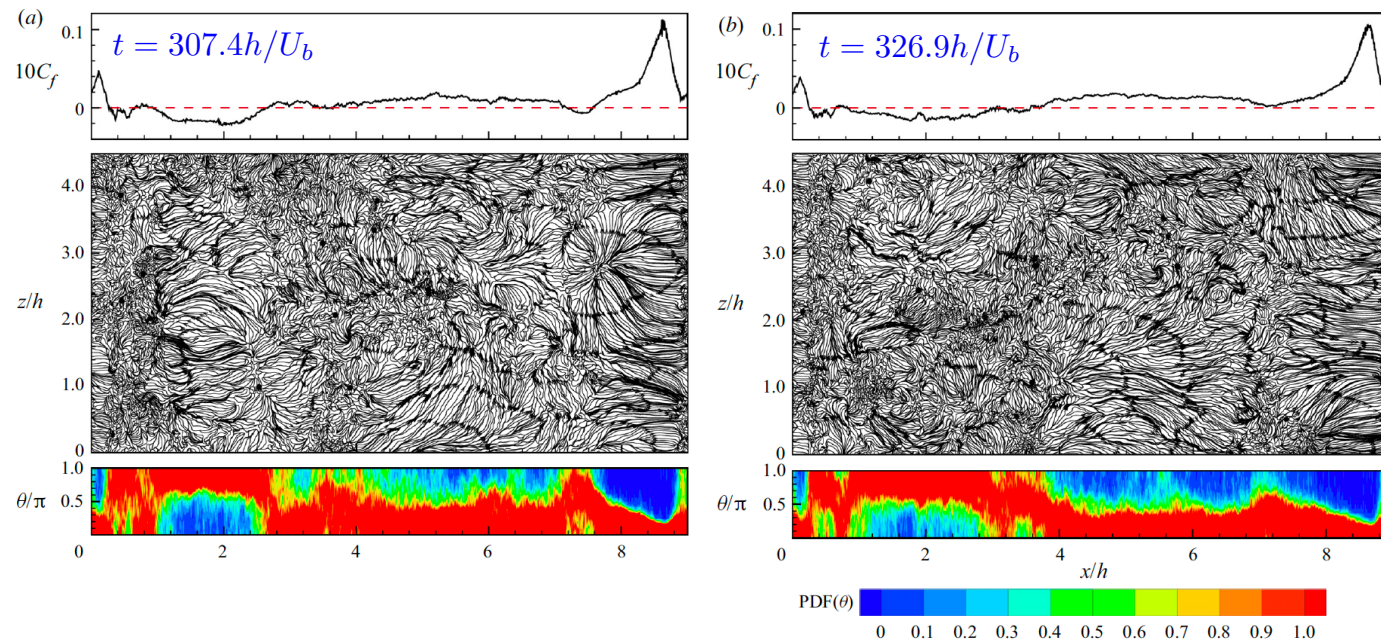
Instantaneous Skin Friction Field: $Re_h=10595$



Instantaneous Skin Friction Field: $Re_h=33000$



Instantaneous Skin Friction Field: $Re_h=10^5$



Conclusion and Future Work

- Wall-bounded turbulent flows may be computed with LES for the “outer” flow and a wall-model for the inner “universal” character
- For WMLES to be predictive **STRONG VALIDATION** is critical
- Stretched spiral SGS model employed for outer LES
- Wall model → ODE for shear stress and Dirichlet BC for velocity at a virtual wall
- Two case studies presented: (a) Airfoils (external) and (b) Periodic hill (internal) with emphasis on validation of “sensitive” quantities such as skin friction and Reynolds stresses
- Future Directions: (a) extend compressible flows, (b) apply to more complex configurations (e.g. NASA CRM – collaboration with Prof. Parsani at KAUST)

Papers on DNS/LES

DNS

- W. Zhang, R. Samtaney, Assessment of spanwise domain size effects on the transitional flow past an airfoil, *Computers and Fluids*, 124:39-53, 2016
- W. Zhang, R. Samtaney, BiGlobal linear stability analysis of low-Re flow past an airfoil at high angle of attack, *Physics of Fluids*, 28(4): 044105, 2016.
- W. Zhang, R. Samtaney, A. Qamar, W. Cheng, W. Gao, Geometrical effects on the airfoil flow separation and transition. *Computer and Fluids*, 116, pp:60-73, 2015
- W. Zhang, R. Samtaney, A direct numerical simulation investigation of the synthetic jet frequency effects on separation control of low-Re flow past an airfoil. *Physics of Fluids*, 27(5): 055101, 2015

WMLES

- W. Cheng, D. I. Pullin, R. Samtaney, Large-eddy simulation of separation and reattachment of a flat plate turbulent boundary layer. *Journal of Fluid Mechanics*, 785, 78-108, 2015
- W. Cheng, R. Samtaney, Power-law versus log-law in wall-bounded turbulence: A large-eddy simulation perspective. *Phys. Fluids*, 26(1), art. no. 011703, 2014

- W. Cheng, R. Samtaney, A high-resolution code for large eddy simulation of incompressible turbulent boundary layer flows. *Computers & Fluids*, 92:82-92, 2013
- W. Gao, W. Zhang, W. Cheng and R. Samtaney, Wall-modeled large eddy simulation of turbulent flow past airfoils. *Journal of Fluid Mechanics*, vol. 873, pp: 174-210, 2019
- W. Gao, W. Cheng and R. Samtaney, Large-Eddy Simulations of Turbulent Flow in a Channel with Streamwise Periodic Constrictions. *Journal of Fluid Mechanics*, to appear, 2020

WRLES

- W.Cheng, D.I.Pullin, R.Samtaney, Large-eddy simulation of Taylor Couette flow at high Reynolds numbers. *Journal of Fluid Mechanics*, vol. 890, A17, 2020.
- W.Cheng, D.I.Pullin, R.Samtaney, Large-eddy simulation of flow over rotating cylinder: the lift crisis at $Re_D=6 \times 10^4$. *Journal of Fluid Mechanics*, 855, pp:371-407, 2018.
- W.Cheng,D.I.Pullin,R.Samtaney,W.Zhang,W.Gao,Large-eddy simulation of flow over cylinder with Re_D from 3.9×10^3 to 8.5×10^5 : a skin friction perspective. *Journal of Fluid Mechanics*, 820:121-158, 2017.
- W.Cheng, D.I.Pullin, R.Samtaney, Large-eddy simulation of flow over a grooved cylinder up to transcritical Reynolds numbers. *Journal of Fluid Mechanics*, 835:327-362, 2017.

Thank you

- Acknowledgement
 - KAUST Office of Competitive Research Funds under Award Number URF/1/1394-1
 - KAUST Supercomputing Laboratory for time on Shaheen II (Cray XC-40) (10s of millions of core hours)
- Questions?